Terrestrial Fluxes of Nutrients and Sediment to Coastal Waters and Their Effects on Coastal Carbon Storage in the Eastern United States

By Brian A. Bergamaschi, Richard A. Smith, Michael J. Sauer, Jhih-Shyang Shih, and Lei Ji

Chapter 6 of
Baseline and Projected Future Carbon Storage and Greenhouse-Gas Fluxes in Ecosystems of the Eastern United States
Edited by Zhiliang Zhu and Bradley C. Reed

Professional Paper 1804

U.S. Department of the Interior
U.S. Geological Survey

U.S. Department of the Interior
SALLY JEWELL, Secretary

U.S. Geological Survey
Suzette M. Kimball, Acting Director

U.S. Geological Survey, Reston, Virginia: 2014

Suggested citation:
Bergamaschi, B.A., Smith, R.A., Sauer, M.J., Shih, J.-S., and Ji, Lei, 2014, Terrestrial fluxes of nutrients and sediment to coastal waters and their effects on coastal carbon storage in the eastern United States, chap. 6 *of* Zhu, Zhiliang, and Reed, B.C., eds., Baseline and projected future carbon storage and greenhouse gas fluxes in ecosystems of the eastern United States: U.S. Geological Survey Professional Paper 1804, p. 85–114, *http://dx.doi.org/10.3133/pp1804*.

ISSN 1044-9612 (print)
ISSN 2330-7102 (online)
ISBN 978-1-4113-3794-7

Contents

6.1. Highlights 85
6.2. Introduction 85
6.3. Coastal Carbon Storage Model 87
6.3.1. Background and Overview 87
6.3.2. Methods and Data 87
6.3.2.1. Terrestrial Flux Model 87
6.3.2.2. Coastal Carbon Storage Model 88
6.4. Results and Discussion 94
6.4.1. Flux of Nutrients, Suspended Sediment, and TOC to Coastal Waters 94
6.4.1.1. Total Nitrogen 94
6.4.1.2. Total Phosphorus 102
6.4.1.3. Total Suspended Sediment 102
6.4.1.4. Total Organic Carbon 102
6.4.2. Carbon Storage in Coastal Waters 109
6.4.2.1. Estuary Retention and Denitrification 109
6.4.2.2. Coastal C_T Storage 109
6.4.2.3. Sediment C_T Inventory 111
6.4.2.4. Projected Changes in C_T Storage in Coastal Waters 112
6.4.3. Summary of Carbon Storage Related to Coastal Processes 113
6.5. Conclusions and Implications 113

Figures

6–1. Map showing the geographic extent of the five regions used in the assessment of coastal carbon storage in the Eastern United States 86
6–2. Maps showing dispersion fields for *A*, nutrients and *B*, sediments in the coastal carbon sequestration model for the Eastern United States 93
6–3. Maps showing *A*, estimated delivered total nitrogen (TN) yield to coastal waters and *B*, major sources of TN in model catchments under baseline (2005) conditions in the Eastern United States 95
6–4. Maps showing difference between estimated delivered total nitrogen (TN) yield to coastal waters under baseline (2005) and projected (2050) conditions for scenarios *A*, A1B and *B*, B1 in the Eastern United States 96
6–5. Maps showing *A*, estimated delivered total phosphorus (TP) yield to coastal waters and *B*, major sources of TP in model catchments under baseline (2005) conditions in the Eastern United States 103
6–6. Maps showing difference between estimated delivered total phosphorus (TP) yield to coastal waters under baseline (2005) conditions and projected (2050) conditions for scenarios *A*, A1B and *B*, B1 in the Eastern United States 104
6–7. Maps showing *A*, estimated delivered total suspended sediment (TSS) yield to coastal waters and *B*, major sources of TSS in model catchments under baseline (2005) conditions in the Eastern United States 105

6–8. Maps showing difference between estimated delivered total suspended sediment (TSS) yield to coastal waters under baseline (2005) conditions and projected (2050) conditions for scenarios *A*, A1B and *B*, B1 in the Eastern United States 106
6–9. Maps showing *A*, estimated delivered total organic carbon (TOC) yield to coastal waters and *B*, major sources of TOC in model catchments under baseline (2005) conditions in the Eastern United States 107
6–10. Maps showing difference between estimated delivered total organic carbon (TOC) yield to coastal waters under baseline (2005) conditions and projected (2050) conditions for scenarios *A*, A1B and *B*, B1 in the Eastern United States 108
6–11. Maps showing model-derived millennial carbon storage rates for carbon storage directly attributable to terrestrial inputs (C_T) in coastal waters *A*, under baseline (2005) conditions and as differences for projected (2050) conditions based on scenarios *B*, A1B and *C*, B1 in the Eastern United States.....110
6–12. Map showing estimated inventory of carbon directly attributable to terrestrial inputs (C_T) that would be stored in the upper 1 meter of sediment under baseline (2005) flux conditions in the Eastern United States 112

Tables

6–1. Variables used in the SPARROW models of total nitrogen, total phosphorous, total suspended sediment, and total organic carbon fluxes in the assessment of coastal carbon storage and fluxes in the Eastern United States 88
6–2. Assumed correspondences between the source categories of the SPARROW model and the LULC classes used in the assessment of coastal carbon storage and fluxes in the Eastern United States.....89
6 –3. Modeled baseline (2005) and projected (2050) estimates of total nitrogen, total phosphorus, total suspended sediment, total organic carbon fluxes to coastal waters, and estimated inventory of carbon in the upper 1 meter of sediment directly attributable to terrestrial inputs in the Eastern United States.....90
6–4. Estimates of total nitrogen, total phosphorous, total suspended sediment, and total organic carbon fluxes to the coastal waters of the Eastern United States by source of the fluxes, under baseline and projected conditions 97

Chapter 6. Terrestrial Fluxes of Nutrients and Sediment to Coastal Waters and Their Effects on Coastal Carbon Storage in the Eastern United States

By Brian A. Bergamaschi,[11] Richard A. Smith,[1] Michael J. Sauer,[1] Jhih-Shyang Shih,[2] and Lei Ji[1]

6.1. Highlights

- Model estimates indicate that nutrient and sediment fluxes from terrestrial environments of the Eastern United States contribute significantly to the uptake and storage of carbon in coastal waters.
- Changes in population and land use are projected to result in significantly greater fluxes of nutrients and sediments to coastal waters by 2050 relative to the baseline years (2001–2005). However, total organic carbon flux to coastal areas is projected to increase only slightly. For example, projected nitrate fluxes for 2050 are 16 to 52 percent higher than the baseline year, depending on the region and LULC scenario modeled. As a consequence, an associated increase in the frequency and duration of coastal and estuarine hypoxia events and harmful algal blooms could be expected.
- The estimated annual coastal carbon storage flux related to continental inputs was 7.9 TgC/yr, or 3 percent of the estimated average annual terrestrial flux based on LULC in 2005.
- Although variable by region, about 60 percent of coastal carbon storage related to terrestrial inputs is buried in sediments and 40 percent is stored in deep ocean waters, below the surface ocean mixed layer.
- Annual rates of coastal carbon storage are projected to increase by 18 to 56 percent between 2005 and 2050, based on several modeled LULC scenarios. This is in contrast to terrestrial rates of carbon storage, which are projected to decrease by 20 percent. The differing trends in coastal and terrestrial storage result from projected increases in nutrient and sediment runoff from urban and agricultural lands and from decreases in forest cover.
- Fluxes of nutrients and sediments from the Eastern United States in 2005 could account for about 9,100 TgC of burial in the active coastal sediment carbon pool (the upper 1 m) and about 6,000 TgC in deep ocean waters. This represents about two thirds of the mass of carbon stored in the major terrestrial carbon pools and is in addition to coastal carbon storage related to oceanic fluxes of nutrients and sediments.

6.2. Introduction

The current and projected LULC maps of the United States that form the centerpiece of the USGS land carbon national assessment (chap. 3) provide a unique opportunity to examine the extent to which LULC affects carbon storage in coastal oceans, given the influence of riverborne fluxes of nutrients and sediments to the coastal oceans, and the role of nutrients and sediments in carbon storage processes. Coastal oceans remove a greater amount of carbon from the atmosphere globally than terrestrial biomass, largely through photosynthetic uptake of atmospheric carbon by phytoplankton and sequestration of this organic material from the surface ocean through either burial in sediments or removal to the deep ocean (Walsh and others, 1985; Hedges and Keil, 1995; Sarmiento and Gruber, 2002; Dunne and others, 2007). More than 90 percent of global phytoplankton productivity occurs in coastal areas of the oceans, in part because of the elevated nutrient supply from terrestrial sources (Smith and Hollibaugh, 1993; Behrenfeld and Falkowski, 1997). These fluxes of sediment from the continents act to sink and bury this phytoplankton production (Milliman and Syvitski, 1992; Armstrong and others, 2001; Dunne and others, 2005; Syvitski and others, 2005). Coastal carbon preservation in sediments is strongly coupled to the availability of nutrients and the sediment supply (Boudreau and Ruddick, 1991; Dagg and others, 2004; Meybeck and others, 2006). Thus, changes in the continental fluxes of nutrients and sediments will affect the coastal storage of carbon.

It is well established that LULC distributions are a primary determinant of terrestrial fluxes of sediments and nutrients to coastal oceans (Seitzinger and others, 2005; Howarth, 2008; Mayorga and others, 2010). It is also well known that both sediment and nutrient delivery to coastal waters has

[1]U.S. Geological Survey

[2]Resources for the Future

been significantly altered by changes in population and land use (Syvitski and others, 2005; da Cunha and others, 2007; Glibert, 2010), resulting in modified patterns of coastal production and carbon burial (Walsh and others, 1985; Rabalais and others, 1996; Leithold and others, 2005; Middelburg and Levin, 2009). This increasing nutrient supply has raised coastal productivity enough to increase commercial fish harvests and to expand the areas where hypoxic conditions occur (Howarth and others, 1996; Nixon and others, 1996; Rabalais and others, 1996; Boyer and others, 2006; Swaney and others, 2012). Continued population growth and increased areal extent and intensity of agricultural lands are expected to accelerate these changes (Syvitski and others, 2005; Mayorga and others, 2010; Seitzinger and others, 2010; Vörösmarty and others, 2010).

The goals of this coastal carbon storage analysis were to evaluate how terrestrial fluxes of sediment and nutrients contribute to carbon storage in the coastal oceans of the Eastern United States and how changing sediment and fluxes associated with different prospective future LULC conditions may alter rates of carbon storage. Terrestrial fluxes of sediment, nutrients, and carbon were quantified for baseline conditions and a range of projected LULC distributions associated with different SRES storylines (chaps. 2 and 3), and the resulting coastal carbon storage for each LULC distribution was inferred using a simple biogeochemical model. These projected changes in terrestrial flux are also useful for assessing potential future coastal water quality conditions (Whitehead and others, 2009), forecasting fish harvests (Oczkowski and Nixon, 2008; Breitburg and others, 2009), gaging the potential for coastal and estuarine hypoxia (Rabalais and others, 2010; Zhang and others, 2010), and evaluating the vulnerability of coastal ecosystems to harmful algal blooms (Glibert and others, 2005; Litchman and others, 2006). The spatially explicit nature of the assessment permits the use of economic models for evaluating and comparing among different policy and land management decisions made to prevent further degradation of aquatic habitats (Paerl, 2006; Shepherd and others, 2007). The coastal carbon storage and burial portion of the assessment will likely help guide scientific studies and monitoring programs in the coastal ocean as well as provide the basis for economic analysis of this important carbon resource (Burdige, 2007; Williams and others, 2009).

Continental flux and coastal carbon storage models were prepared for baseline LULC and projected future LULC under SRES scenarios A1B, A2, and B1 (chaps. 2 and 3) to explore a range of potential effects of LULC on carbon flux and storage. The geographic extent of the coastal assessment was from the northern border to the southern border of the Eastern United States and was divided into the Great Lakes, Gulf of Maine, Mid-Atlantic Bight, South Atlantic Bight, and Gulf of Mexico regions (fig. 6–1). The model includes all the watersheds that drain from these regions into the adjacent coastal waters, composing the majority of the continental United States. The coastal carbon storage model considers only coastal processes affected by the terrestrial nutrients and sediments delivered to coastal waters within a particular region, with an arbitrary offshore oceanic boundary at the 2,000-m isobath.

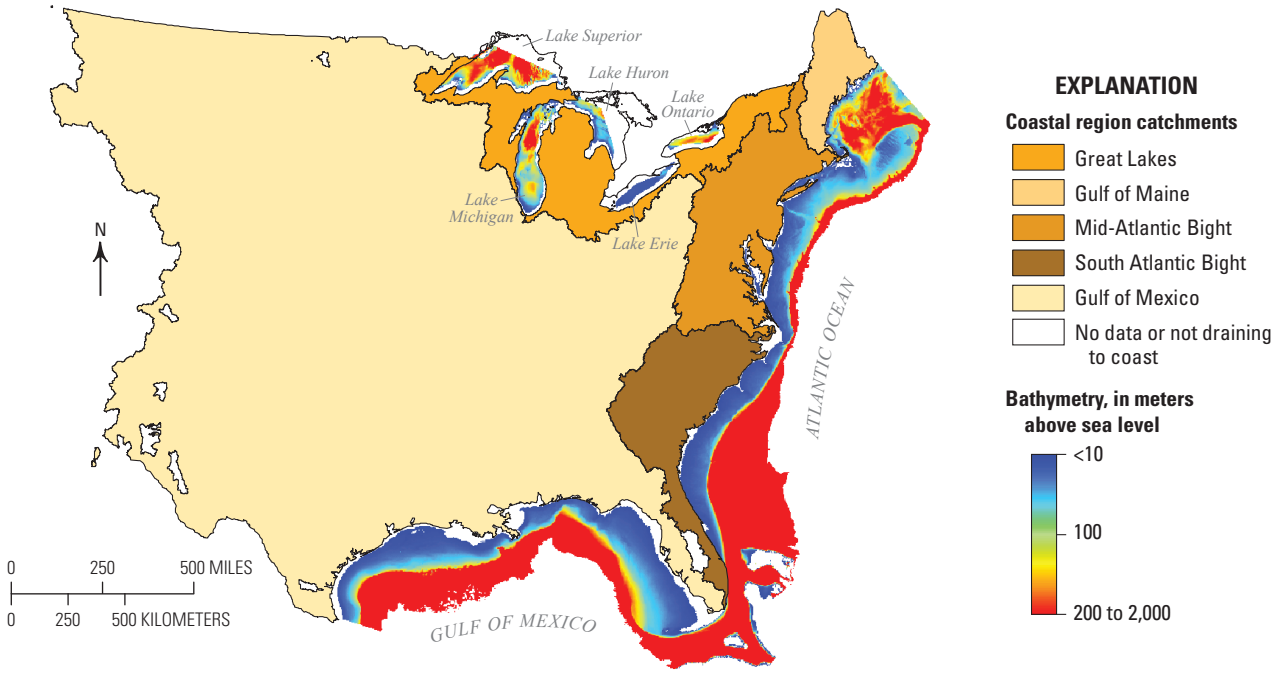

Figure 6–1. Map showing the geographic extent of the five regions used in the assessment of coastal carbon storage in the Eastern United States. The geographic extent of the regions includes all catchments in the Eastern United States draining to waters of the Atlantic Ocean, the Gulf of Mexico, and the Great Lakes and extends in coastal waters to a water depth of 2,000 meters (m). Catchment areas within the model domain that do not drain to the coast or have insufficient data to accurately model are indicated.

6.3. Coastal Carbon Storage Model

6.3.1. Background and Overview

The analysis described in this chapter comprises two distinct modeling efforts. One assesses the riverine fluxes of nutrients and sediments to coastal waters and changes caused by changing LULC, and a separate one assesses the effect those fluxes may have on carbon storage in coastal waters, as well as how carbon storage may change under scenarios of altered terrestrial fluxes.

The first model relies on the databases described in chapter 3 of this report that document present and future projected LULC under different SRES scenarios (A1B, A2, and B1). For the baseline LULC and for the projected LULC for each scenario in 2050, riverine fluxes of TOC, total nitrogen (TN), total phosphorus (TP), and total suspended sediment (TSS) to coastal waters were estimated using the hybrid statistical-mechanical Spatially Referenced Regression on Watershed Attributes (SPARROW) model (Smith and others, 1997; Schwarz and others, 2006). The SPARROW model consists of regressions of large water quality datasets to LULC, process-based mass-transport components for water flow paths and in-stream processing, and mass-balance constraints (Schwarz and others, 2006). Relations between land use and flux are statistically robust, provided water quality records used for model development cover a sufficient length of time and include accurate streamflow measurements (Cohn and others, 1992). The SPARROW model is routinely used for regional assessments of contaminant sources and fluxes and is now a routine part of the USGS water-quality assessment activities (Preston and others, 2011). The advantage of using the SPARROW model is that it permits assessment using projected future LULC and population conditions. Results from the SPARROW model based on SRES storylines and spatially detailed modeling represent an important product of this analysis because they project changes in loads of nutrients and sediment to estuaries and coastal areas and may be useful in separate assessments of water quality for a range of potential future conditions.

The second part of this analysis uses a simple heuristic biogeochemical model to assess the potential magnitude of coastal carbon storage directly associated with the riverine fluxes of sediments, carbon, and nutrients. The model structure follows that of Dunne and others (2007), who demonstrated that the rate of carbon burial in shallow ocean waters may be much higher than previously recognized. The goal of the coastal model is to provide the basis for comparing coastal carbon storage estimates associated with baseline and projections of individual SRES scenarios. To permit such a comparison, the model was developed to provide estimates of millennial carbon storage associated with a single year of riverine inputs under different scenarios. This approach necessarily involves evaluation of the flux of a single year through processes occurring over timescales of days to weeks (for example, primary production), months to decades (for example, sediment transport), and decades to centuries (for example, carbon burial). Given this construct, the coastal model is intended to be representational rather than realistic and focuses specifically on how LULC may be related to coastal carbon storage. The model makes no attempt to reproduce or project coastal ocean carbon cycling and does not account for carbon cycling and carbon storage associated with upwelling, downwelling, advective transport of carbon, and other oceanic processes. It should be noted that the carbon storage estimates provided by the model represent only a fraction of the total carbon stored in coastal sediments.

For the purpose of this analysis, carbon storage is defined as burial in coastal sediments below the zone of pore-water oxygen penetration or removal of carbon from the surface ocean across the maximum depth of the upper mixed layer and away from contact with the atmosphere. Separate components of the model estimate retention of nutrients and sediment in estuaries, "new production" of phytoplankton biomass, transit and degradation of biomass through the water column, and burial of biomass in sediments or loss below the deep mixed layer into the deep ocean, depending on the location of the original biomass production. It also estimates the amount of terrestrial TOC stored. Because the amount of surface productivity that is eventually stored depends largely on the depth of the water column and the sediment burial rate, carbon storage in coastal areas is sensitive to the spatial distribution of nutrients and sediments in the surface waters. The model presented here uses a spatial distribution developed from averaged remote sensing data to represent the physical processes leading to spatial variability in coastal waters.

Climate-related changes, such as those to river discharge and vegetation, were not estimated in the LULC coverages and thus were not part of this analysis. The potential effects of climate change on nutrients or biological processes in the coastal ocean also were not included. Although changing climate would be expected to have some influence on future fluxes of nutrients and suspended sediment to coastal waters, LULC is expected to be the main driver of the variability in these parameters between 2005 and 2050 (Allan, 2004). Potential effects of temperature rise on TN flux can be estimated from the characteristics of the temperature term in the SPARROW TN model (Alexander and others, 2008). For example, the TN flux from a typical watershed in the Eastern United States was projected to decrease by 13 percent because of increased denitrification associated with the higher temperature for an air temperature increase of 2 °C between 2005 and 2050. The effects of temperature on TP, TSS, and TOC flux would be expected to be smaller. Effects of changing streamflow on nutrients and sediment are more difficult to anticipate given the large current uncertainty about the direction and magnitude of changes in the hydrologic cycle in the Eastern United States (Najjar and others, 2000, 2010)

6.3.2. Methods and Data

6.3.2.1. Terrestrial Flux Model

Estimates of TN, TP, TSS, and TOC fluxes were prepared for the baseline year and for SRES scenarios A1B, A2, and B1

for 2050 using SPARROW models calibrated to 1992 LULC conditions (see chap. 3 for description of modeling of LULC changes from 2005 through 2050). SPARROW models describe the steady-state balance between contaminant supply rates and average streamflow and water quality conditions (Schwarz and others, 2006; Shih and others, 2010; Smith and others, 1997). Use of the TN, TP, TSS, and TOC models to project fluxes through 2050 assumes that contaminant sources change in accordance with projected LULC scenarios and that water quality conditions reach a new steady state based on current streamflow rates.

Modeled estimates of TSS, TN, TP, and TOC fluxes were produced for 2,174 tributary drainages to the Great Lakes and the east and gulf coasts of the United States. Estimates of TOC that were produced using a different modeling approach (chap. 5) agree with those presented here.

For surface-water monitoring stations that had sufficient data on discharge and water quality, water-quality parameters were estimated by spatially correlating the stream data with georeferenced data on the constituent sources (for example, atmospheric deposition, fertilizers, human and animal wastes) and delivery factors (for example, precipitation, topography, vegetation, soils, and water routing). Parameter estimation ensured that the calibrated model would not be more complex than can be supported by the data.

SPARROW models describe mass transport in watersheds as three sequential processes—(1) source supply, (2) land-to-water transport, and (3) channel-network transport (Smith and others, 1997). Data describing these processes are developed on a stream reach and associated catchment basis. There are about 63,000 reaches or catchments in the national-scale dataset used to calibrate the models. Table 6–1 provides information on the TN, TP, TSS, and TOC models used in this assessment to quantify the flux of material to coastal waters.

The source variables (table 6–1) were of particular importance because they served as the basis for translating the baseline and projected LULC into coastal delivery of TOC, TN, TP, and TSS from 2005 through 2050. Table 6–2 summarizes the correspondence between the LULC classes and the source categories from the SPARROW model. An underlying assumption made in modeling projected changes in coastal flux was that the rate of the source supply will change in proportion to the LULC changes in each modeled catchment. The change in the value of the population variable in the TN model within each catchment was approximated by the projected change in the developed land area (chap. 3). The modeled SRES scenarios are thus reflected in the LULC and SPARROW modeling (chaps. 2 and 3; Sohl and others, 2012b).

The 90-percent confidence intervals for the coastal flux estimates in table 6–3 were developed through a bootstrap procedure in which 200 equally likely estimates for each entry in the table were randomly generated based on the error characteristics of the model determined during calibration. The width of the confidence intervals surrounding the 1992 and 2050 flux estimates includes coefficient and residual (that is, model specification) errors (Schwarz and others, 2006). The residual errors of the flux estimates for individual coastal rivers within each region were assumed to reflect idiosyncrasies of the river watersheds. However, the estimated errors surrounding the "percent-change" estimates for each coastal river were assumed to arise only from coefficient error, based on the further assumption that the idiosyncrasies of a given river can be assumed to be the same in 2005 and 2050. Thus, the confidence intervals for the percent-change estimates are smaller than those for the separate 2005 and 2050 flux estimates.

6.3.2.2. Coastal Carbon Storage Model

The approach used for modeling coastal processes for storing carbon was based largely on the model approach of Dunne and others (2007) that captured the fate of surface productivity as it moves through the water column and into the deep ocean and sediments. This model approach was adapted to analyze only the sensitivity of carbon storage associated with the potential new production that results from terrestrial inputs from the Eastern United States.

Table 6–1. Variables used in the SPARROW models of total nitrogen, total phosphorous, total suspended sediment, and total organic carbon fluxes in the assessment of coastal carbon storage and fluxes in the Eastern United States.

[R^2, coefficient of determination; SPARROW, spatially referenced regressions of watershed attributes water-quality model; TN, total nitrogen; TP, total phosphorus; TSS, total suspended solids; TOC, total organic carbon]

Model	Number of sites	R^2	Source variables	Reference
TN	425	0.933	Population, atmospheric nitrate deposition, corn or soybean fertilizer, alfalfa fertilizer, wheat fertilizer, other crop fertilizer, farm animal waste, forest, barren land, shrubland	Alexander and others (2008)
TP	425	0.871	Population, corn or soybean fertilizer, alfalfa fertilizer, other crop fertilizer, farm animal waste, forest, barren land (transitional), shrubland	Alexander and others (2008)
TSS	1,828	0.711	Urban area, forest, crop and pasture land, federal land, other marginal land, channel storage and erosion	Schwarz (2008)
TOC	1,125	0.928	Cultivated land, pasture, deciduous forest, evergreen forest, mixed forest, rangeland, urban land, wetlands, in-stream photosynthesis	Shih and others (2010)

Table 6–2. Assumed correspondences between the source categories of the SPARROW model and the LULC classes used in the assessment of coastal carbon storage and fluxes in the Eastern United States.

[See chapter 3 of this report for definitions of the land use and land cover (LULC) classes. NA, not available; SPARROW, spatially referenced regressions of watershed attributes water-quality model]

Model source	LULC class
Total nitrogen (TN) model	
Population	Developed land
Fertilizer nitrogen applied to agriculture	Agriculture
Forest	Deciduous, evergreen, mixed forests
Nitrogen content of farm animal waste	Grassland and shrubland
Barren land	Barren land
Shrubland	Shrubland
Atmospheric nitrate (NO_3) deposition	Separate deposition layer; future changes assumed proportional to developed land
Total phosphorus (TP) model	
Population	Developed land
Fertilizer phosphorous applied to agriculture	Agriculture
Forest	Deciduous, evergreen, mixed forests
Phosphorous content of farm animal waste	Grassland and shrubland
Barren land	Barren land
Shrubland	Shrubland
Total suspended solids (TSS) model	
Developed land	Developed land
Crop and pasture land	Agriculture
Forest	Deciduous, evergreen, mixed forests
Federally managed land	Barren land, grassland and shrubland
Other land	Barren land, grassland and shrubland
Stream channels	No LULC correspondence; assumed to be constant
Total organic carbon (TOC) model[1]	
Developed land	Developed land
Cultivated land	Agriculture
Deciduous forest	Deciduous forest
Evergreen forest	Evergreen forest
Mixed forest	Mixed forest
Rangeland	Grassland and shrubland
Wetlands	Herbaceous and woody wetland
Pasture	Hay/pasture

[1]The TOC model includes in-stream photosynthesis as a TOC source which does not correspond directly to a LULC class. However, the in-stream photosynthesis estimates depend, in part, on predictions from the TP model, which does incorporate the LULC classes, as indicated in this table.

The model is a simple heuristic one-dimensional model of productivity, carbon burial in sediments, and deep water remineralization implemented with a 4-km resolution over the 10- to 2,000-m bathymetry of the coastal oceans and Great Lakes of the Eastern United States. A 4-km model resolution was used to correspond with the spatial resolution of the remote sensing imagery and used to establish a realistic spatial distribution of nutrients and sediments in the coastal ocean.

A representative spatial field for production and for sediment dispersion in the coastal ocean was developed from a composite image of chlorophyll a (Chl *a*) and of total suspended sediment (TSS) derived from European Space Agency medium resolution imaging spectrometer (MERIS) data at nominal 4-km resolution for the entire coastal waters of the United States in 2011. The Chl2 algorithm from MERIS was specifically used to avoid overestimation of Chl *a* due to colored dissolved organic matter present in nearshore coastal zones where typical empirical ocean color algorithms fail (for example, algorithms OC4 and OC3 from the SeaWiFS Data Analysis System (SeaDAS); Szeto and others, 2011; Sauer and others, 2012; Siegel and others, 2013). The resulting ocean color imagery was divided into study regions and aligned with NOAA ETOPO1 bathymetry. Loading to each pixel in the model domain was estimated by unit-normalizing the integrated value across the region and multiplying by the input mass to that region.

The purpose of the remote sensing imagery is to conceptualize coastal physical dynamics in the model while

Table 6–3. Modeled baseline (2005) and projected (2050) estimates of total nitrogen, total phosphorus, total suspended sediment, total organic carbon fluxes to coastal waters, and estimated inventory of carbon in the upper 1 meter of sediment directly attributable to terrestrial inputs in the Eastern United States.

[Data in parentheses are 90-percent confidence intervals. Projected (2050) conditions are based on Intergovernmental Panel on Climate Change Special Report on Emissions Scenarios (SRES; Nakićenović and others, 2000) scenarios A1B, A2, and B1. Values may not add to totals shown due to independent rounding. CI, confidence intercval; Tg/yr, teragrams per year; kg/km^2/yr, kilograms per square kilometer per year; km^2, square kilometers; —, no data]

A. Fluxes and yields—Continued								
Region	Baseline, 2005 estimate (90-percent CI)		Scenario A1B		Scenario A2		Scenario B1	
	Flux, in Tg/yr	Yield, in kg/km^2/yr	Projected (2050), in Tg/yr	Percentage change	Projected (2050), in Tg/yr	Percentage change	Projected (2050), in Tg/yr	Percentage change
Total nitrogen								
Great Lakes	0.3 (0.1–0.8)	888 (326–2,280)	0.4 (0.1–0.9)	22.9 (22.6–23.1)	0.4 (0.1–0.9)	21.1 (20.8–21.4)	0.4 (0.1–0.8)	15.7 (15.4–15.9)
Gulf of Maine	0.1 (0.0–0.1)	505 (168–1,094)	0.1 (0.0–0.2)	32.7 (32.1–33.3)	0.1 (0.0–0.2)	42.5 (41.5–43.5)	0.4 (0.2–1.0)	22.2 (21.8–22.7)
Mid-Atlantic Bight	0.4 (0.1–0.8)	1,030 (401–2,318)	0.5 (0.2–1.1)	31.2 (30.9–31.4)	0.5 (0.2–1.0)	28.2 (28.9–28.5)	0.2 (0.1–0.4)	20.6 (20.3–20.8)
South Atlantic Bight	0.1 (0.1–0.3)	473 (169–1,114)	0.2 (0.1–0.5)	51.0 (50.6–51.4)	0.2 (0.1–0.5)	45.3 (44.9–45.7)	0.1 (0.0–0.2)	26.1 (25.7–26.5)
Gulf of Mexico	1.8 (0.7–4.1)	375 (149–643)	2.2 (0.8–4.9)	19.3 (19.0–19.6)	2.1 (0.8–4.9)	17.7 (17.4–17.9)	2.1 (0.8–4.8)	16.8 (16.5–17.0)
Total	**2.7 (1.0–6.0)**	**450 (175–1,019)**	**3.3 (1.3–7.5)**	**23.3 (23.0–23.6)**	**3.2 (1.2–7.4)**	**21.5 (21.2–21.8)**	**3.2 (1.2–7.2)**	**17.8 (17.5–18.0)**
Total phosphorus								
Great Lakes	0.0 (0.0–0.0)	59 (0–89)	0.0 (0.0–0.0)	12.3 (12.0–12.5)	0.0 (0.0–0.0)	9.6 (9.4–9.8)	0.0 (0.0–0.0)	5.8 (5.6–5.9)
Gulf of Maine	0.0 (0.0–0.0)	34 (0–84)	0.0 (0.0–0.0)	11.5 (11.2–11.8)	0.0 (0.0–0.01	18.2 (17.5–18.9)	0.0 (0.0–0.0)	5.1 (5.0–5.2)
Mid-Atlantic Bight	0.0 (0.0–0.1)	86 (29–172)	0.0 (0.0–0.1)	15.1 (14.9–15.3)	0.0 (0.0–0.1)	13.3 (13.1–13.5)	0.0 (0.0–0.1)	8.7 (8.6–8.9)
South Atlantic Bight	0.0 (0.0–0.0)	34 (0–101)	0.0 (0.0–0.0)	19.7 (19.4–20.0)	0.0 (0.0–0.0)	17.8 (17.4–18.1)	0.0 (0.0–0.0)	7.9 (7.7–8.2)
Gulf of Mexico	0.3 (0.1–0.4)	52 (10–87)	0.3 (0.1–0.4)	2.0 (2.0–2.0)	0.3 (0.1–0.4)	1.4 (1.4–1.4)	0.3 (0.1–0.4)	0.6 (0.6–0.7)
Total	**0.3 (0.1–0.6)**	**54 (10–93)**	**0.3 (0.1–0.6)**	**4.7 (4.6–4.8)**	**0.3 (0.1–0.6)**	**3.9 (3.9–4.0)**	**0.3 (0.1–0.6)**	**2.1 (2.0–2.1)**
Total suspended solids								
Great Lakes	12.8 (0.4–39.8)	37,769 (1,243–11,7943)	15.7 (0.5–49.4)	23.4 (22.9–23.9)	15.1 (0.5–47.5)	18.7 (18.4–19.0)	13.9 (0.5–43.4)	9.0 (8.8–9.3)
Gulf of Maine	3.0 (0.1–8.5)	25,397 (673–71,707)	3.3 (0.1–9.3)	10.1 (9.7–10.5)	3.3 (0.1–9.5)	10.7 (10.3–11.1)	3.1 (0.1–8.9)	4.2 (4.0–4.3)
Mid-Atlantic Bight	25.6 (0.8–70.9)	73,103 (2,175–202,772)	32.2 (1.0–91.5)	26.2 (25.5–26.8)	31.1 (0.9–88.2)	21.8 (21.2–22.3)	28.5 (0.9–80.1)	11.7 (11.3–12.1)
South Atlantic Bight	13.5 (0.4–43.4)	45,395 (1,350–146,346)	20.6 (0.6–67.7)	52.8 (51.3–54.3)	19.5 (0.6–63.9)	44.9 (43.6–46.2)	16.8 (0.5–55.2)	25.0 (24.1–25.8)
Gulf of Mexico	361.6 (5.5–920.0)	74,900 (1,133–190,568)	453.7 (7.3–1,199.1)	25.5 (24.2–26.8)	424.9 (6.6–1,120.7)	17.5 (16.6–18.4)	429.2 (6.6–1134.9)	18.7 (17.7–19.7)
Total	**416.4 (7.1–1,082.6)**	**70,214 (1,204–182,560)**	**525.6 (9.5–1,416.9)**	**26.2 (24.9–27.5)**	**494.0 (8.8–1,329.6)**	**18.6 (17.8–19.5)**	**491.6 (8.5–1132.4)**	**18.1 (17.1–19.0)**

Table 6–3. Modeled baseline (2005) and projected (2050) estimates of total nitrogen, total phosphorus, total suspended sediment, total organic carbon fluxes to coastal waters, and estimated inventory of carbon in the upper 1 meter of sediment directly attributable to terrestrial inputs in the Eastern United States.—Continued

[Data in parentheses are 90-percent confidence intervals. Projected (2050) conditions are based on Intergovernmental Panel on Climate Change Special Report on Emissions Scenarios (SRES; Nakićenović and others, 2000) scenarios A1B, A2, and B1. Values may not add to totals shown due to independent rounding. CI, confidence intercval; Tg/yr, teragrams per year; kg/km^2/yr, kilograms per square kilometer per year; km^2, square kilometers; —, no data]

A. Fluxes and yields—Continued

Region	Baseline, 2005 estimate (90-percent CI)		Scenario A1B		Scenario A2		Scenario B1	
	Flux, in Tg/yr	Yield, in kg/km^2/yr	Projected (2050), in Tg/yr	Percentage change	Projected (2050), in Tg/yr	Percentage change	Projected (2050), in Tg/yr	Percentage change
			Total organic carbon					
Great Lakes	1.3 (0.5–2.7)	3,709 (1,480–7,964)	1.3 (0.5–2.8)	2.8 (2.7–2.8)	1.3 (0.5–2.8)	2.8 (2.8–2.9)	1.3 (0.5–2.8)	2.3 (2.3–2.4)
Gulf of Maine	0.3 (0.1–0.7)	2,862 (1,094–6,144)	0.4 (0.1–0.8)	1.9 (1.8–1.9)	0.4 (0.1–0.7)	2.4 (2.4–2.5)	0.4 (0.1–0.7)	0.8 (0.7–0.8)
Mid-Atlantic Bight	1.5 (0.6–3.1)	4,201 (1,631–8,870)	1.6 (0.6–3.3)	5.9 (5.8–6.0)	1.5 (0.6–3.2)	4.5 (4.4–4.6)	1.5 (0.6–3.2)	3.5 (3.5–3.6)
South Atlantic Bight	1.7 (0.7–3.8)	5,665 (2,228–12,825)	1.8 (0.7–4.0)	5.7 (5.6–5.8)	1.8 (0.7–3.9)	4.0 (3.9–4.1)	1.8 (0.7–4.0)	6.3 (6.2–6.3)
Gulf of Mexico	13.7 (5.5–29.6)	2,830 (1,148–6,139)	13.8 (5.6–29.9)	1.0 (0.9–1.0)	13.8 (5.6–30.0)	1.2 (1.2–1.3)	14.2 (5.8–30.7)	3.8 (3.8–3.9)
Total	**18.4 (7.4–40.0)**	**3,104 (1,250–6,738)**	**18.8 (7.6–40.7)**	**1.9 (1.9–2.0)**	**18.8 (7.6–40.7)**	**1.9 (1.8–1.9)**	**19.1 (7.7–41.4)**	**3.9 (3.8–3.9)**

B. Total terrestrial carbon storage

Region	Drainage area, in km^2	Sediment C_T inventory, in TgC	Baseline (2005), in Tg/y	Scenario A1B		Scenario A2		Scenario B1	
				Projected (2050), in Tg/yr	Percentage change	Projected (2050), in Tg/yr	Percentage change	Projected (2050), in Tg/yr	Percentage change
Great Lakes	337,789	2,900	0.4 (0.0–1.3)	0.5 (0.0–1.7)	31	0.5 (0.0–1.6)	27.5	0.5 (0.1–1.5)	18.6
Gulf of Maine	118,817	1,200	0.1 (0.0–0.2)	0.1 (0.0–0.3)	33.8	0.1 (0.0–0.3)	42.3	0.1 (0.0–0.3)	22.1
Mid-Atlantic Bight	349,505	1,400	0.7 (0.1–1.9)	1.0 (0.2–2.6)	35.8	1.0 (0.2–2.5)	32	0.9 (0.1–2.4)	22.3
South Atlantic Bight	296,285	1,300	0.5 (0.2–1.2)	0.7 (0.2–1.8)	55.7	0.7 (0.2–1.7)	49.2	0.6 (0.2–1.5)	28.5
Gulf of Mexico	4,827,771	2,300	6.2 (1.6–17.8)	7.5 (1.9–18.5)	21.3	7.3 (1.9–18.1)	19	7.3 (1.8–18.0)	18.4
Total	**5,930,167**	**9,100**	**7.8 (1.8–22.4)**	**9.8 (2.3–24.9)**	**25.4**	**9.6 (2.3–24.7)**	**22.7**	**9.3 (2.3–24.0)**	**19.4**

still permitting use of the one-dimensional carbon storage modeling framework across the model domain. There is no horizontal transport in the model. This is an oversimplification that neglects to account in any way for processes not present in the composite images, such as near-bottom cross shelf transport of sediment and carbon (Hales and others, 2008). However, explicitly modeling the effects of physical dynamics is beyond the scope of this analysis.

The model input for the coastal portion of the analysis was the output from the SPARROW fluxes to estuaries and

coastal areas, modified to account for nutrient and sediment retention in estuaries and for direct diffusive denitrification of nitrate from coastal waters in coastal sediments. Direct coastal erosion is not included in the analysis, but nutrient and sediment fluxes from the land surface adjacent to coasts and estuaries are included in the SPARROW model output from the modeling scenarios that were run for this assessment even if the coasts and estuaries are not part of a watershed included in the database. Nutrient retention in estuaries was estimated separately for nitrogen and phosphorus according to the global relations presented by Nixon and others (1996) and the residence time estimates in the NOAA National Estuarine Eutrophication Assessment (NEEA) estuaries database (*http://ian.umces.edu/neea/siteinformation.php*). Sediment retention was assumed to be similar to phosphorus retention. No retention was assumed for the Mississippi River because of the discharge geometry and the time scale of the analysis. This assumption was necessary because no models exist for long-term carbon burial in estuaries, and estuaries are subject to substantial reworking of sedimentary carbon on decadal time scales (Keil and others, 1997).

Denitrification is a strong sink for nitrogen in the coastal oceans, resulting in a loss of nitrogen potentially available to support photosynthetic production (Nixon and others, 1996; Seitzinger and Giblin, 1996), with the bulk of removal occurring through either denitrification during remineralization of organic matter or direct denitrification of nitrate in the overlying water. Separate approaches were used to account for each of these processes in the model. Before calculating primary production, the demand from shallow water column and direct denitrification was removed from the totalized TN mass as an inverse geometric function of water depth and TN concentration. The shallow water TN demand used in the model ranged from 1,200 millimoles per square meter per year ($mmol/m^2/yr$) in shallow waters to 6 $mmol/m^2/yr$ at 200 m. Denitrification during remineralization within the sediments was accounted for by assuming that organic nitrogen from new production arriving at the sediment surface is either buried or denitrified and thus was not available to support additional primary production in the surface waters (Murray and Parslow, 1999; Piña-Ochoa and Alvarez-Cobelas, 2006). Phosphate was assumed to be liberated by remineralization and consequently was not found to be limiting to modeled production.

Following reduction of TSS mass estimated by the SPARROW model for estuary retention, the resulting lower TSS mass was converted to pixel loadings across each region by multiplying the total input mass by each normalized pixel value of the TSS MERIS images across the 30- to 2,000-m bathymetry (fig. 6–2). For the purpose of this assessment, it was assumed that no net sediment deposition (or carbon burial) occurred at mean water depths less than 30 m over time scales of decades, owing to sediment resuspension and transport due to wind waves, internal waves, storms, and flood events (Blair and others, 2004).

Nutrient loading to each pixel was established using the unit normalized satellite Chl *a* imagery (fig 6–2) multiplied by the adjusted input mass of TN. Due to the denitrification demand, TN distribution was performed in two iterations. In the first iteration, the TN mass adjusted for retention by estuaries was distributed across the 10- to 2,000-m bathymetry for the purpose of calculating the diffusive and shallow water denitrification demand (see below). After the calculation and removal of TN lost through these processes, a second iteration redistributed the remainder of the TN mass across the 30- to 2,000-m bathymetry.

Nutrient inputs to the surface ocean were assumed to be converted by photosynthetic activity into "new production" according to the stoichiometric balance described by Anderson and Sarmiento (1994), where the ratio of carbon to nitrogen is 7:1 and the ratio of carbon to phosphorus is 117:1. Nutrients released into the surface waters during water-column remineralization were assumed to be available to support additional new production.

The fate of this modeled new production depended on the depth of the water column and the deep mixed layer. The deep mixed layer was assigned a uniform thickness of 200 m, based on the statistical analysis of global ocean annual maximum mixed layer depths (Kara and others, 2000; de Boyer Montégut and others, 2004). New production in areas with water column depths shallower than 200 m was presumed to undergo the process of sediment burial, with remineralized CO_2 equilibrated with the atmosphere. Where water depths exceeded 200 m, new production sank out of the deep mixed layer, and the carbon and associated nutrients were considered removed from the surface ocean and stored in the deep ocean. Remineralization of new production below the mixed layer was modeled using the relationship derived by the Martin curve (Martin and others, 1987) as employed in Dunne and others (2007), yielding a fraction of new production that is subject to burial in sediments and a fraction that is stored as dissolved inorganic carbon in the deep ocean. However, because there is no millennial deep-water reservoir of carbon in the Great Lakes, all carbon storage in the Eastern United States is presumed to be through sediment burial and all CO_2 resulting from remineralization presumed equilibrated with the atmosphere.

Nutrients supporting new organic production were presumed to regenerate until fully consumed and removed from the mixed layer by sinking or to the sediments. Once new production was removed to the sediments, it was not considered buried until it was buried below the zone of oxygen penetration and resistant to remineralization over millennial timescales (Hedges and Keil, 1995; Dunne and others, 2007). Burial of the fraction of material arriving at the sediment surface was estimated using the empirical formulation of Dunne and others (2007, equation 2), using data from Alperin and others (2002), Thomas and others (2002), and Hofmann and others (2011). Organic carbon of terrestrial origin was assumed to be 5 percent of the total carbon buried (Blair and others, 2003; Burdige, 2005). Terrestrial carbon buried in sediments represents about 0.4 percent of the SPARROW-estimated terrestrial TOC flux under baseline conditions. All

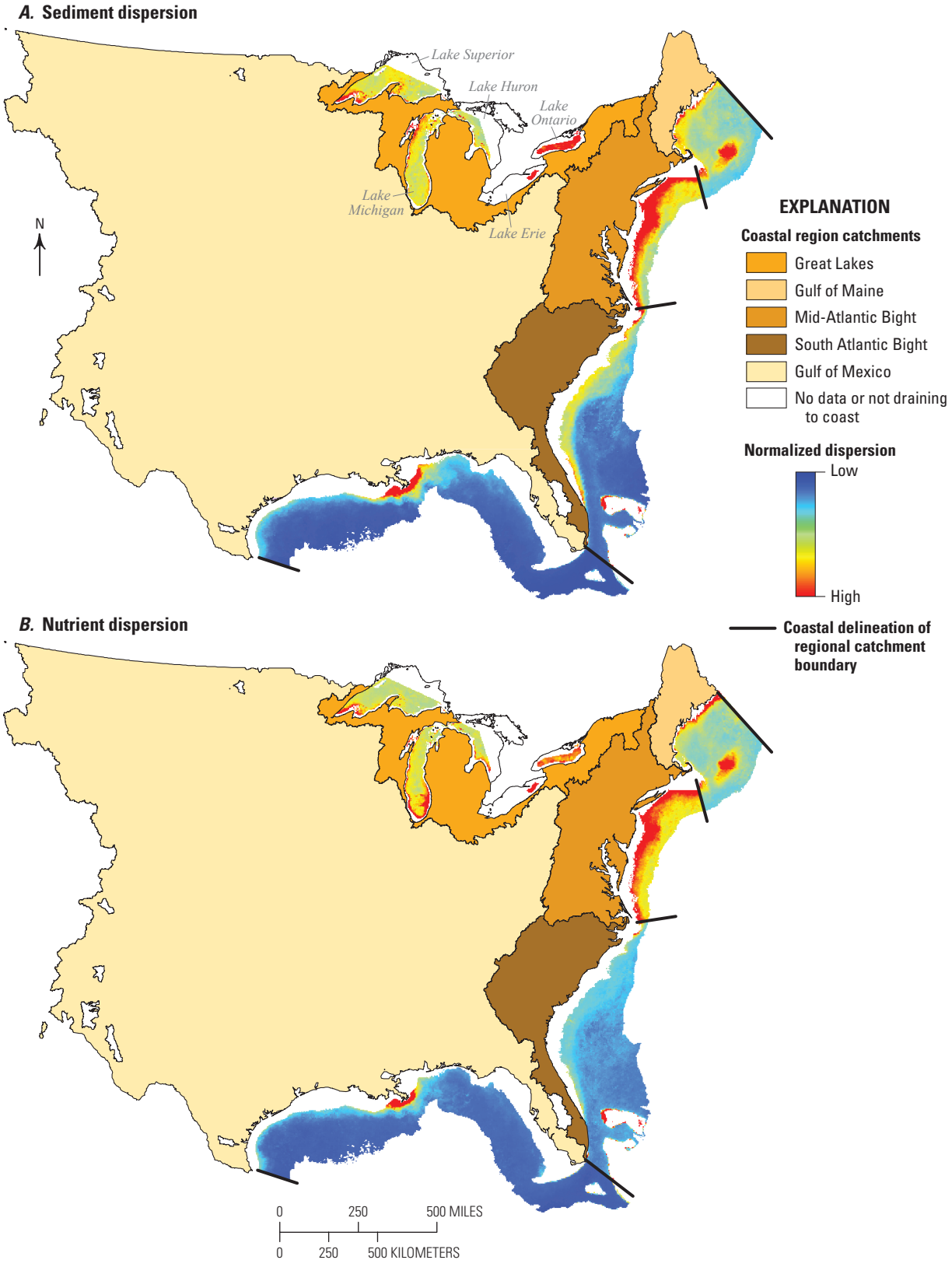

Figure 6–2. Maps showing dispersion fields for *A*, nutrients and *B*, sediments in the coastal carbon sequestration model for the Eastern United States. Heavy black lines indicate the boundaries between the Great Lakes, east coast, and Gulf of Mexico.

remaining TOC mass that originates from terrestrial flux is presumed remineralized in the surface ocean and the resulting CO_2 equilibrated with the atmosphere (Hedges and Keil, 1995; Hedges and others, 1997).

The effects of increased hypoxia on carbon burial were not considered; generally, increased hypoxia results in higher rates of organic carbon preservation (Bergamaschi and others, 1997; Green and others, 2006). Thus, carbon storage in this model is defined as the rate at which carbon fixed by new production is either buried to the extent that it escapes remineralization over millennial timescales or is exported to the deep ocean where it is buried or prevented from equilibration with the atmosphere over timescales of ocean circulation. Burial was calculated over the entire model domain, whereas carbon was stored in deep ocean waters only where water depths exceed the depth of the permanent mixed layer.

To permit comparison to terrestrial carbon stocks and to assess the process of long-term sediment carbon accumulation, the amount of carbon that would accumulate in the upper 1 m of sediments due to the modeled storage rates was estimated by applying the organic content derived from the model to the upper meter of sediment, assuming a porosity of 0.7 and a density of 2.5 grams per cubic meter (g/cm^3; Dunne and others, 2007). The organic content was given by dividing the carbon burial rate by the sediment mass accumulation rate. It should be noted that this heuristic calculation yields a result for the conditions of the modeled year (2005) although the timescale of accumulation of the upper 1 m of sediment can span thousands of years.

6.4. Results and Discussion

The primary active pools of carbon storage in the oceans are organic carbon buried in surficial sediment and dissolved inorganic carbon in seawater (Hedges and Keil, 1995; Sarmiento and Gruber, 2002). This study focuses exclusively on how nutrient and sediment fluxes from terrestrial environments affect carbon storage within both these pools. To understand the model results, the carbon derived from terrestrial process must be clearly distinguished from carbon derived from other processes that store carbon in the coastal ocean, such as primary production supported by nutrients from the deep ocean (Sarmiento and Gruber, 2002). The model presented here tracks the fraction of carbon associated with primary production that is specifically supported by nutrients from the continents (terrestrial carbon; C_T) and ultimately estimate the fraction of this carbon eventually stored in the coastal ocean through either the transport and burial of that primary production by riverborne sediments or through the transport to the deep ocean, with both processes isolating carbon from the atmosphere for millennial timescales. The symbol C_T is introduced here to distinguish this subset of terrestrially supported carbon from the much larger carbon pool in the ocean.

6.4.1. Flux of Nutrients, Suspended Sediment, and TOC to Coastal Waters

Sources in common for TN and TP include treated municipal sewage, industrial wastewater, urban runoff, and crop and animal agricultural activity. Although the atmosphere contributes significant amounts of TN, it is a negligible source of TP in most watersheds. Principal sources for TSS are erosion and channel scour as well as urban, crop, and pasture lands. The principal source for TOC is in-stream photosynthesis, followed by wetlands and cultivated lands.

6.4.1.1. Total Nitrogen

The SPARROW model estimated a baseline TN flux of 2.7 Tg/yr (fig. 6–3; table 6–3) for the Eastern United States. About two thirds of the total flux originated in the Gulf of Mexico drainage, nearly one quarter originated in the east coast drainages, and about one tenth originated in the Great Lakes drainage. However, after adjusting for drainage area, the flux per unit area (yield) of TN in the Gulf of Mexico drainage was lowest among the five regions (table 6–3). This reflects the much longer distances nitrogen must travel to the Gulf of Mexico from sources in the large Mississippi Basin, which leads to elevated losses of TN to denitrification in stream and river channels. By contrast, the highest yields of TN came from the Mid-Atlantic Bight part of the east coast drainages (Gulf of Maine, Mid-Atlantic Bight, and South Atlantic Bight) where urban, agricultural, and atmospheric sources are high and travel distances to the east coast are relatively short.

The estimated TN flux from all five coastal regions was projected to increase significantly by 2050 under all three SRES scenarios (fig. 6–4; table 6–3), primarily because of increasing population and resulting increases in atmospheric sources of CO_2 in those areas (table 6–4). Under scenarios A1B and A2, U.S. and global population and per-capita income were projected to increase substantially by 2050. Although U.S. agricultural production was expected to increase substantially to meet elevated worldwide demand, the increase was assumed to occur largely through increases in yield rather than in agricultural land area. The estimated TN flux from all five regions was projected to increase by more than 20 percent in scenarios A1B and A2, with increases in the South Atlantic Bight region alone projected to increase by 45 percent and 51 percent, respectively (figs. 6–3 and 6–4; table 6–3). By contrast, under scenario B1, a greater focus on biodiversity protection than under scenarios A1B and A2 results in a smaller rise in the land area devoted to urban development, despite increases in population and wealth. Hence, TN flux to the five coastal regions of the Eastern United States is projected to increase by smaller percentages under scenario B1 than under scenario A1B or A2.

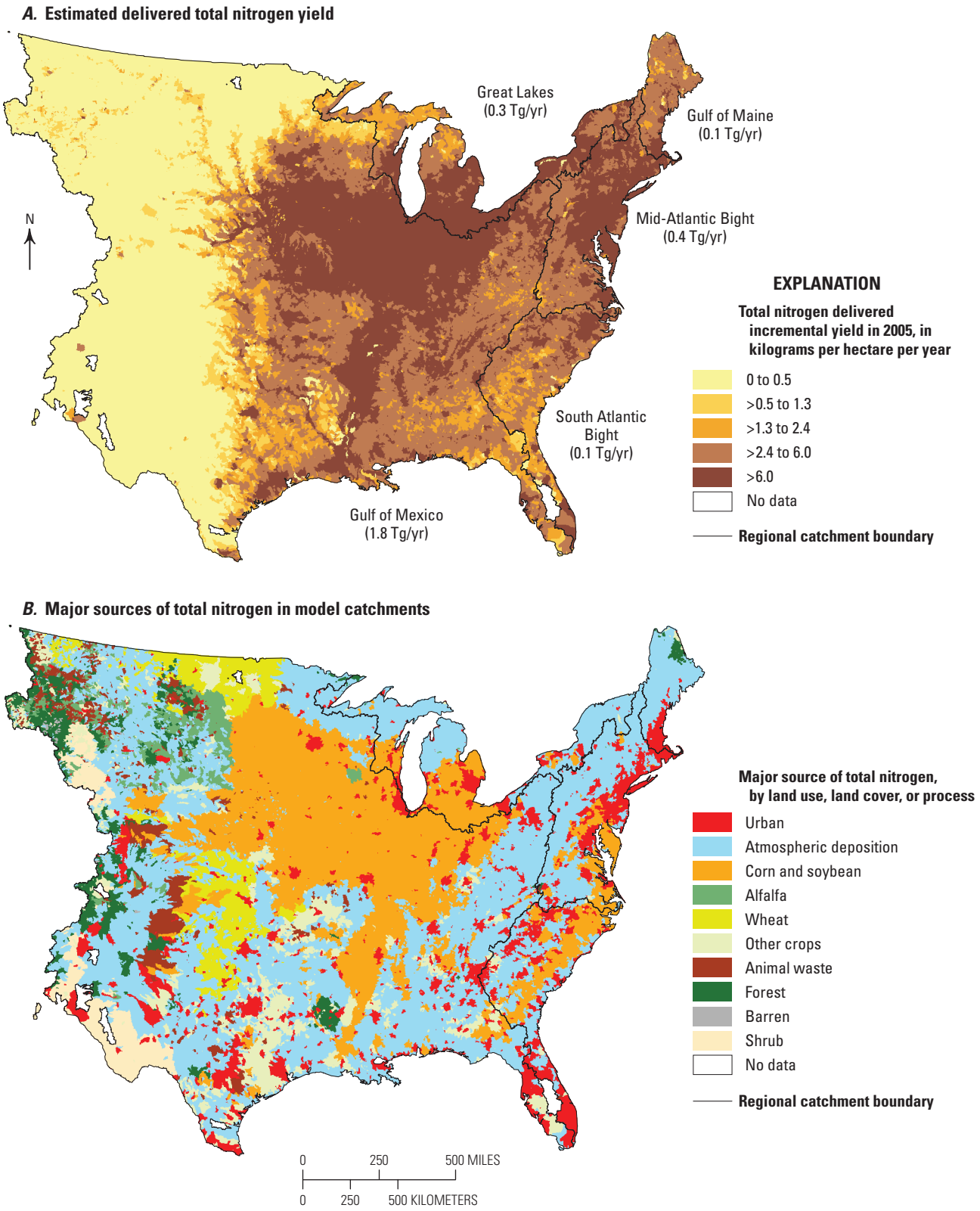

Figure 6–3. Maps showing *A*, estimated delivered total nitrogen (TN) yield to coastal waters and *B*, major sources of TN in model catchments under baseline (2005) conditions in the Eastern United States. Delivered yield reflects the effects of in-stream losses that occur during transport from the outlet of a catchment through the stream and river system to coastal waters. Values shown in parentheses indicate net flux of TN for each region. LULC, land cover and land use; Tg/yr, teragrams per year; >, more than.

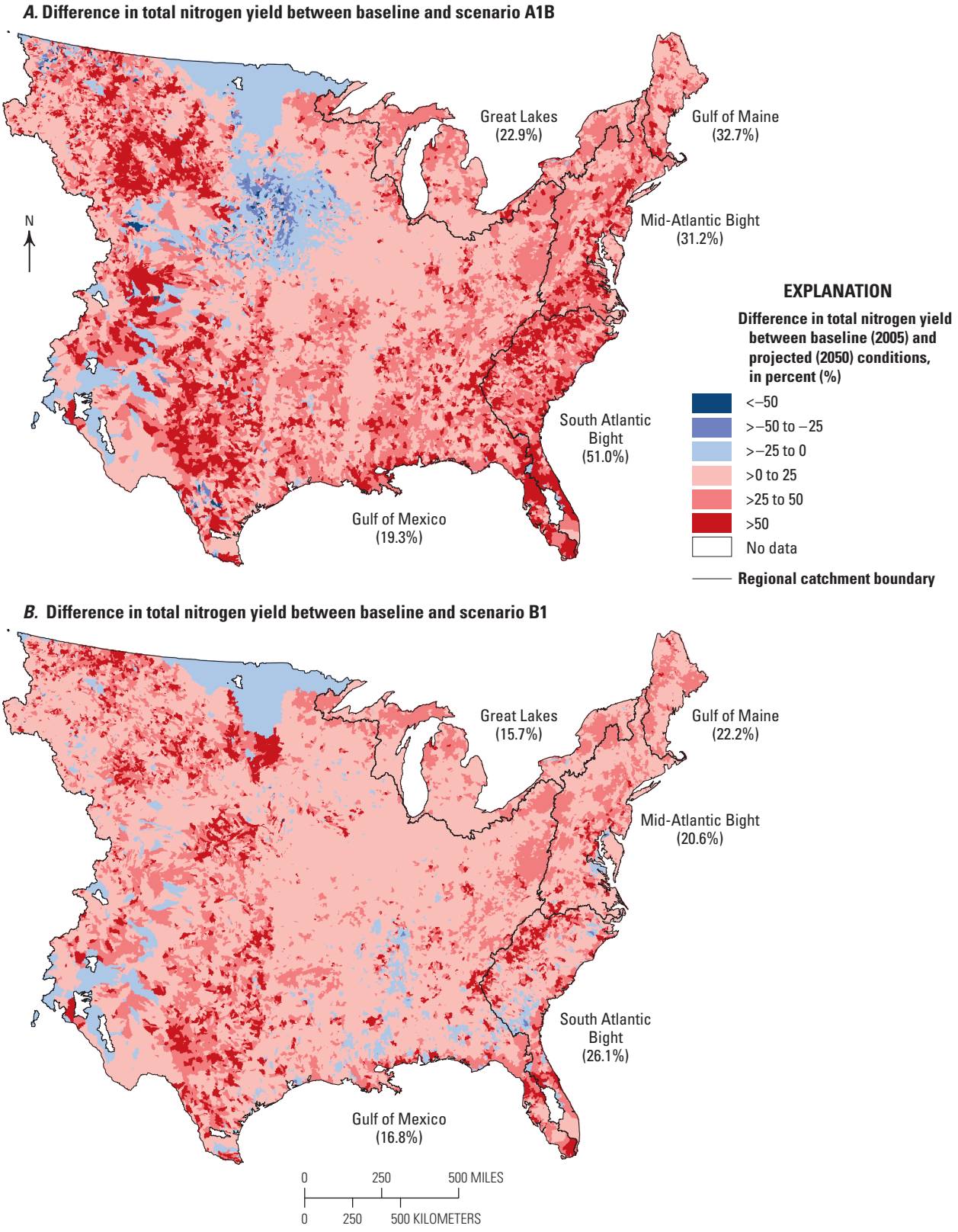

Figure 6–4. Maps showing difference between estimated delivered total nitrogen (TN) yield to coastal waters under baseline (2005) and projected (2050) conditions for Intergovernmental Panel on Climate Change Special Report on Emissions Scenarios (SRES; Nakićenović and others, 2000) scenarios *A*, A1B and *B*, B1 in the Eastern United States. Values shown in parentheses indicate regional difference from baseline. <, less than; >, more than.

Table 6–4. Estimates of total nitrogen, total phosphorous, total suspended sediment, and total organic carbon fluxes to the coastal waters of the Eastern United States by source of the fluxes, under baseline and projected conditions.

[Projected (2050) conditions are based on Intergovernmental Panel on Climate Change Special Report on Emissions Scenarios (SRES; Nakićenović and others, 2000) scenarios A1B, A2, and B1. Data may not add to totals shown due to independent rounding. Gg/yr, billion grams per year]

Source	Baseline (2005)	Scenario A1B		Scenario A2		Scenario B1	
		2050	Change in mass	2050	Change in mass	2050	Change in mass
Great Lakes							
Total nitrogen (TN)							
Population	78.1	117.7	39.6	107.7	29.7	97.6	19.6
Atmospheric deposition	69.5	102.9	33.4	102.9	33.4	102.9	33.4
Corn and soybean	94.8	93.1	–1.8	96.0	1.1	91.8	–3.0
Alfalfa	16.4	16.5	0.2	17.5	1.1	15.6	–0.7
Wheat	9.1	8.9	–0.1	9.2	0.1	8.9	–0.2
Other crops	15.5	15.8	0.3	16.9	1.4	14.8	–0.7
Farm animal waste	4.6	3.8	–0.8	3.6	–0.9	3.8	–0.7
Forest	15.2	13.8	–1.5	13.4	–1.8	15.2	0.0
Barren land	0.1	0.1	0.0	0.1	0.0	0.1	0.0
Shrubland	0.0	0.0	0.0	0.0	0.0	0.0	0.0
Total	**303.3**	**372.6**	**69.3**	**367.2**	**64.0**	**350.8**	**47.5**
Total phosphorus (TP)							
Population	7.7	10.9	3.2	10.1	2.4	9.3	1.6
Corn and soybean	3.3	3.0	–0.3	3.1	–0.2	3.1	–0.2
Alfalfa	2.4	2.2	–0.2	2.4	–0.1	2.3	–0.2
Other crops	1.6	1.5	–0.1	1.6	0.0	1.5	–0.1
Farm animal waste	0.9	0.7	–0.2	0.7	–0.2	0.7	–0.2
Forest	1.7	1.5	–0.2	1.4	–0.3	1.6	0.0
Barren land	0.0	0.0	0.0	0.0	0.0	0.0	0.0
Shrubland	0.0	0.0	0.0	0.0	0.0	0.0	0.0
Total	**17.6**	**19.8**	**2.2**	**19.3**	**1.7**	**18.6**	**1.0**
Total suspended solids (TSS)							
Urban	4,401.9	7,463.3	3,061.4	6,606.7	2,204.8	5,761.5	1,359.6
Forest	138.2	121.3	–16.9	115.5	–22.7	137.6	–0.7
Federal land	13.9	13.6	–0.3	13.5	–0.4	13.5	–0.3
Crop and pasture land	4,676.2	4,636.0	–40.2	4,898.5	222.3	4,490.7	–185.4
Grassland, shrubland, barren land	92.6	75.6	–17.0	72.9	–19.7	74.1	–18.4
Channel storage or erosion	3,435.1	3,435.1	0.0	3,435.1	0.0	3,435.1	0.0
Total	**12,757.9**	**15,744.8**	**2,987.0**	**15,142.2**	**2,384.3**	**13,912.6**	**1,154.7**
Total organic carbon (TOC)							
Cultivated land	183.8	183.5	–0.3	190.7	6.9	177.3	–6.5
Deciduous forest	81.6	81.6	0.0	81.6	0.0	81.6	0.0
Evergreen forest	20.5	20.5	0.0	20.5	0.0	20.5	0.0
Mixed forest	51.1	51.1	0.0	51.1	0.0	51.1	0.0
Urban land	65.8	102.1	36.3	93.0	27.2	83.7	17.9
Wetlands	729.7	728.2	–1.6	731.0	1.3	747.5	17.7
In-stream photosynthesis	120.2	120.2	0.0	120.2	0.0	120.2	0.0
Total	**1,252.7**	**1,287.1**	**34.4**	**1,288.2**	**35.4**	**1,281.9**	**29.2**

Table 6–4. Estimates of total nitrogen, total phosphorous, total suspended sediment, and total organic carbon fluxes to the coastal waters of the Eastern United States by source of the fluxes, under baseline and projected conditions.—Continued

[Projected (2050) conditions are based on Intergovernmental Panel on Climate Change Special Report on Emissions Scenarios (SRES; Nakićenović and others, 2000) scenarios A1B, A2, and B1. Data may not add to totals shown due to independent rounding. Gg/yr, billion grams per year]

Source	Baseline (2005)	Scenario A1B		Scenario A2		Scenario B1	
		2050	Change in mass	2050	Change in mass	2050	Change n mass
Gulf of Maine							
Total nitrogen (TN)							
Population	18.6	24.7	6.2	23.8	5.3	21.6	3.1
Atmospheric deposition	21.0	31.1	10.1	31.1	10.1	31.1	10.1
Corn and soybean	0.7	0.8	0.1	1.2	0.4	0.6	–0.1
Alfalfa	0.6	0.7	0.1	1.0	0.4	0.6	–0.1
Wheat	0.0	0.0	0.0	0.0	0.0	0.0	0.0
Other crops	3.3	7.3	4.0	13.5	10.2	3.7	0.4
Farm animal waste	0.3	0.3	0.0	0.3	0.0	0.3	0.0
Forest	13.6	12.3	–1.3	12.1	–1.5	13.3	–0.3
Barren land	0.3	0.3	0.0	0.3	0.0	0.3	0.0
Shrubland	0.1	0.1	0.0	0.1	0.0	0.1	0.0
Total	**58.5**	**77.7**	**19.2**	**83.4**	**24.9**	**71.5**	**13.0**
Total phosphorus (TP)							
Population	2.5	3.2	0.6	3.1	0.6	2.9	0.4
Corn and soybean	0.0	0.0	0.0	0.0	0.0	0.0	0.0
Alfalfa	0.1	0.1	0.0	0.1	0.0	0.1	0.0
Other crops	0.2	0.5	0.2	0.9	0.7	0.2	0.0
Farm animal waste	0.1	0.1	0.0	0.1	0.0	0.1	0.0
Forest	1.7	1.4	–0.3	1.3	–0.4	1.6	–0.1
Barren land	0.2	0.1	0.0	0.1	0.0	0.2	0.0
Shrubland	0.0	0.0	0.0	0.0	0.0	0.0	0.0
Total	**4.8**	**5.3**	**0.5**	**5.7**	**0.9**	**5.0**	**0.2**
Total suspended solids (TSS)							
Urban	637.5	915.7	278.1	852.3	214.7	778.5	141.0
Forest	113.2	102.1	–11.1	99.8	–13.4	110.6	–2.6
Federal land	3.6	3.6	0.0	3.6	0.0	3.6	0.0
Crop and pasture land	173.8	210.6	36.8	295.1	121.3	159.8	–14.0
Grassland, shrubland, barren land	158.9	160.3	1.4	159.7	0.8	160.2	1.3
Channel storage or erosion	1,930.6	1,930.6	0.0	1,930.6	0.0	1,930.6	0.0
Total	**3,017.6**	**3,322.8**	**305.2**	**3,341.0**	**323.4**	**3,143.3**	**125.7**
Total organic carbon (TOC)							
Cultivated land	6.9	8.4	1.5	11.4	4.5	6.4	–0.6
Deciduous forest	26.6	26.6	0.0	26.6	0.0	26.6	0.0
Evergreen forest	35.7	35.7	0.0	35.7	0.0	35.7	0.0
Mixed forest	83.3	83.3	0.0	83.3	0.0	83.3	0.0
Urban land	21.6	29.2	7.5	28.0	6.4	25.5	3.8
Wetlands	135.0	132.4	–2.6	132.4	–2.6	134.4	–0.7
In-stream photosynthesis	34.3	34.3	0.0	34.3	0.0	34.3	0.0
Total	**343.6**	**350.0**	**6.4**	**351.9**	**8.3**	**346.2**	**2.6**

Table 6–4. Estimates of total nitrogen, total phosphorous, total suspended sediment, and total organic carbon fluxes to the coastal waters of the Eastern United States by source of the fluxes, under baseline and projected conditions.—Continued

[Projected (2050) conditions are based on Intergovernmental Panel on Climate Change Special Report on Emissions Scenarios (SRES; Nakićenović and others, 2000) scenarios A1B, A2, and B1. Data may not add to totals shown due to independent rounding. Gg/yr, billion grams per year]

Source	Baseline (2005)	Scenario A1B		Scenario A2		Scenario B1	
		2050	Change in mass	2050	Change in mass	2050	Change n mass
Mid-Atlantic Bight							
Total nitrogen (TN)							
Population	170.1	242.2	72.2	226.4	56.3	214.2	44.1
Atmospheric deposition	84.3	124.7	40.5	124.7	40.5	124.7	40.5
Corn and soybean	50.9	52.8	1.9	54.5	3.6	45.1	–5.8
Alfalfa	11.4	11.5	0.2	13.3	1.9	10.1	–1.2
Wheat	5.1	5.5	0.4	5.4	0.3	4.5	–0.6
Other crops	16.1	17.4	1.3	19.7	3.6	14.2	–1.9
Farm animal waste	0.5	0.6	0.0	0.4	–0.1	0.5	–0.1
Forest	25.5	22.6	–2.9	22.2	–3.3	25.3	–0.2
Barren land	0.1	0.1	0.0	0.1	0.0	0.1	0.0
Shrubland	0.0	0.0	0.0	0.0	0.0	0.0	0.0
Total	**364.0**	**477.6**	**113.5**	**466.9**	**102.8**	**438.9**	**74.8**
Total phosphorus (TP)							
Population	19.7	26.1	6.4	24.9	5.2	23.8	4.1
Corn and soybean	2.0	1.8	–0.1	1.9	0.0	1.7	–0.3
Alfalfa	2.3	2.0	–0.3	2.3	0.0	1.9	–0.5
Other crops	1.4	1.3	–0.1	1.5	0.1	1.2	–0.2
Farm animal waste	0.1	0.1	0.0	0.1	0.0	0.1	0.0
Forest	4.5	3.2	–1.3	3.3	–1.2	4.0	–0.5
Barren land	0.1	0.1	0.0	0.1	0.0	0.1	0.0
Shrubland	0.0	0.0	0.0	0.0	0.0	0.0	0.0
Total	**30.1**	**34.7**	**4.6**	**34.1**	**4.0**	**32.7**	**2.6**
Total suspended solids (TSS)							
Urban	9,559.2	15,903.7	6,344.4	13,980.6	4,421.3	13,500.6	3,941.3
Forest	693.0	617.9	–75.2	602.6	–90.4	693.8	0.8
Federal land	7.6	7.6	0.0	7.6	0.0	7.6	0.0
Crop and pasture land	8,072.5	8,486.9	414.4	9,306.2	1,233.7	7,110.3	–962.2
Grassland, shrubland, barren land	44.8	45.8	1.0	43.5	–1.3	43.5	–1.3
Channel storage or erosion	7,173.1	7,173.1	0.0	7,173.1	0.0	7,173.1	0.0
Total	**25,550.3**	**32,234.9**	**6,684.7**	**31,113.5**	**5,563.3**	**28,528.9**	**2,978.6**
Total organic carbon (TOC)							
Cultivated land	117.0	124.6	7.7	133.1	16.1	103.5	–13.4
Deciduous forest	134.4	134.4	0.0	134.4	0.0	134.4	0.0
Evergreen forest	39.6	39.6	0.0	39.6	0.0	39.6	0.0
Mixed forest	132.7	132.7	0.0	132.7	0.0	132.7	0.0
Urban land	155.1	236.9	81.8	219.5	64.4	202.8	47.8
Wetlands	557.8	555.0	–2.8	543.8	–14.0	575.5	17.7
In-stream photosynthesis	331.6	331.6	0.0	331.6	0.0	331.6	0.0
Total	**1,468.3**	**1,554.9**	**86.6**	**1,534.7**	**66.4**	**1,520.3**	**52.0**

Table 6–4. Estimates of total nitrogen, total phosphorous, total suspended sediment, and total organic carbon fluxes to the coastal waters of the Eastern United States by source of the fluxes, under baseline and projected conditions.—Continued

[Projected (2050) conditions are based on Intergovernmental Panel on Climate Change Special Report on Emissions Scenarios (SRES; Nakićenović and others, 2000) scenarios A1B, A2, and B1. Data may not add to totals shown due to independent rounding. Gg/yr, billion grams per year]

Source	Baseline (2005)	Scenario A1B		Scenario A2		Scenario B1	
		2050	Change in mass	2050	Change in mass	2050	Change n mass
South Atlantic Bight							
Total nitrogen (TN)							
Population	54.5	108.1	53.6	101.7	47.2	85.4	30.9
Atmospheric deposition	29.3	43.3	14.1	43.3	14.1	43.3	14.1
Corn and soybean	29.9	35.1	5.2	33.5	3.7	25.7	–4.2
Alfalfa	0.4	0.5	0.1	0.5	0.1	0.3	–0.1
Wheat	4.3	4.9	0.6	4.8	0.5	3.7	–0.7
Other crops	12.2	13.9	1.7	13.5	1.3	9.8	–2.4
Farm animal waste	0.7	0.6	–0.1	0.6	–0.1	0.7	–0.1
Forest	11.1	8.9	–2.2	9.4	–1.8	11.0	–0.1
Barren land	0.7	0.7	0.0	0.7	0.0	0.7	0.0
Shrubland	0.0	0.0	0.0	0.0	0.0	0.0	0.0
Total	**143.2**	**216.2**	**73.0**	**208.1**	**64.9**	**180.6**	**37.4**
Total phosphorus (TP)							
Population	6.3	10.0	3.8	9.8	3.5	8.7	2.4
Corn and soybean	2.1	2.2	0.1	2.1	0.0	1.7	–0.4
Alfalfa	0.2	0.1	0.0	0.2	0.0	0.1	0.0
Other crops	1.8	1.8	0.0	1.8	–0.1	1.4	–0.5
Farm animal waste	0.5	0.5	–0.1	0.4	–0.1	0.5	0.0
Forest	2.2	1.4	–0.8	1.5	–0.7	1.9	–0.2
Barren land	0.9	0.7	–0.2	0.7	–0.1	0.8	–0.1
Shrubland	0.0	0.0	0.0	0.0	0.0	0.0	0.0
Total	**14.0**	**16.7**	**2.8**	**16.5**	**2.5**	**15.1**	**1.1**
Total suspended solids (TSS)							
Urban	4,515.8	11,150.3	6,634.5	10,092.2	5,576.4	8,424.2	3,908.4
Forest	314.3	253.9	–60.4	261.4	–52.8	309.2	–5.1
Federal land	5.1	5.0	–0.1	5.0	–0.1	5.0	–0.1
Crop and pasture land	3,128.1	3,655.9	527.7	3,643.7	515.5	2,583.7	–544.5
Grassland, shrubland, barren land	562.2	562.6	0.4	561.7	–0.5	561.8	–0.5
Channel storage or erosion	4,925.0	4,925.0	0.0	4,925.0	0.0	4,925.0	0.0
Total	**13,450.5**	**20,552.6**	**7,102.1**	**19,489.0**	**6,038.5**	**16,808.7**	**3,358.2**
Total organic carbon (TOC)							
Cultivated land	93.8	107.7	13.9	103.9	10.1	76.9	–16.9
Deciduous forest	49.2	49.2	0.0	49.2	0.0	49.2	0.0
Evergreen forest	93.3	93.3	0.0	93.3	0.0	93.3	0.0
Mixed forest	64.2	64.2	0.0	64.2	0.0	64.2	0.0
Urban land	85.3	177.9	92.6	167.6	82.3	141.2	56.0
Wetlands	977.7	966.6	–11.2	952.6	–25.2	1,043.7	66.0
In-stream photosynthesis	315.0	315.0	0.0	315.0	0.0	315.0	0.0
Total	**1,678.5**	**1,773.8**	**95.3**	**1,745.8**	**67.3**	**1,783.5**	**105.0**

Table 6–4. Estimates of total nitrogen, total phosphorous, total suspended sediment, and total organic carbon fluxes to the coastal waters of the Eastern United States by source of the fluxes, under baseline and projected conditions.—Continued

[Projected (2050) conditions are based on Intergovernmental Panel on Climate Change Special Report on Emissions Scenarios (SRES; Nakićenović and others, 2000) scenarios A1B, A2, and B1. Data may not add to totals shown due to independent rounding. Gg/yr, billion grams per year]

Source	Baseline (2005)	Scenario A1B		Scenario A2		Scenario B1	
		2050	Change in mass	2050	Change in mass	2050	Change n mass
Gulf of Mexico							
Total nitrogen (TN)							
Population	250.8	463.1	212.3	416.1	165.4	366.1	115.3
Atmospheric deposition	330.7	489.5	158.8	489.5	158.8	489.5	158.8
Corn and soybean	791.9	756.1	–35.7	777.4	–14.4	815.8	23.9
Alfalfa	47.1	46.4	–0.7	48.2	1.1	49.4	2.3
Wheat	60.1	60.8	0.7	61.3	1.2	63.0	2.9
Other crops	168.4	184.8	16.4	184.3	15.9	167.1	–1.3
Farm animal waste	58.3	64.7	6.4	59.0	0.7	58.0	–0.3
Forest	87.8	77.3	–10.5	78.1	–9.7	88.7	0.9
Barren land	1.4	1.4	0.0	1.4	0.0	1.4	0.0
Shrubland	8.6	9.5	0.9	8.7	0.1	8.6	0.0
Total	**1,805.1**	**2,153.7**	**348.5**	**2,124.2**	**319.0**	**2,107.6**	**302.5**
Total phosphorus (TP)							
Population	48.6	74.7	26.1	69.5	20.9	64.6	16.0
Corn and soybean	51.6	44.7	–6.9	47.2	–4.3	49.2	–2.3
Alfalfa	22.2	18.9	–3.2	20.4	–1.7	21.0	–1.2
Other crops	29.9	28.3	–1.6	29.0	–0.8	26.8	–3.0
Farm animal waste	61.5	60.2	–1.2	58.4	–3.1	56.2	–5.3
Forest	31.1	23.1	–8.0	23.9	–7.2	28.9	–2.2
Barren land	1.2	1.1	–0.1	1.1	–0.1	1.1	–0.1
Shrubland	4.9	4.9	0.0	4.7	–0.2	4.5	–0.4
Total	**250.8**	**255.8**	**5.0**	**254.3**	**3.5**	**252.4**	**1.6**
Total suspended solids (TSS)							
Urban	76,076.7	146,043.3	69,966.5	128,042.0	51,965.3	118,550.3	42,473.6
Forest	5,230.3	4,497.7	–732.6	4,613.0	–617.3	5,247.7	17.3
Federal land	4,484.5	4,958.9	474.4	4,654.5	170.0	4,533.0	48.5
Crop and pasture land	160,678.3	158,912.7	–1,765.6	162,415.7	1,737.4	180,778.6	20,100.3
Grassland, shrubland, barren land	26,362.3	50,535.4	24,173.1	36,394.9	10,032.7	31,333.3	4,971.0
Channel storage or erosion	88,768.5	88,768.5	0.0	88,768.5	0.0	88,768.5	0.0
Total	**361,600.6**	**453,716.5**	**92,115.8**	**424,888.7**	**63,288.0**	**429,211.4**	**67,610.7**
Total organic carbon (TOC)							
Cultivated land	1,771.5	1,771.0	–0.5	1,802.4	30.9	1,879.5	108.1
Deciduous forest	550.0	550.0	0.0	550.0	0.0	550.0	0.0
Evergreen forest	277.7	277.7	0.0	277.7	0.0	277.7	0.0
Mixed forest	441.7	441.7	0.0	441.7	0.0	441.7	0.0
Urban land	385.5	694.4	308.9	633.6	248.1	560.6	175.1
Wetlands	3,694.6	3,520.1	–174.5	3,585.6	–109.0	3,936.5	241.9
In-stream photosynthesis	6,544.0	6,544.0	0.0	6,544.0	0.0	6,544.0	0.0
Total	**13,664.9**	**13,798.8**	**133.9**	**13,834.9**	**170.0**	**14,189.9**	**525.0**

6.4.1.2. Total Phosphorus

The results for TP flux to coastal waters followed a generally similar pattern to those for TN, reflecting similar environmental sources. The total baseline (2005) flux of TP from the five regions was 0.3 Tg/yr (figs. 6–5 and 6–6; table 6–3), with 79 percent originating in the Gulf of Mexico drainage, 15 percent originating in the combined east coast drainages, and 6 percent originating in the Great Lakes drainage. Again, the mid-Atlantic Bight part of the east coast drainage had the highest yield of the three regions of the east coast due to large sources from urban and agricultural lands and relatively short travel distances to the east coast. In contrast to the pattern for TN yield, however, the Mid-Atlantic Bight TP yield was not dramatically larger than that from the gulf coast drainage. This is because, whereas atmospheric sources of TN were especially high in the Mid-Atlantic Bight, atmospheric sources of TP were negligible in both regions.

The estimated TP flux from all five coastal regions was projected to increase between 2005 and 2050 under all three future projection scenarios (fig. 6–6; table 6–3), but only minimally so for some regions and scenarios. Most notably, TP flux from the Gulf of Mexico drainage was projected to increase by only 2.0 percent, 1.4 percent, and 0.6 percent under scenarios A1B, A2, and B1, respectively, during the 45 years of study (fig. 6–6; table 6–3). By contrast, TP flux from the South Atlantic Bight drainage was projected to increase by 19.7 percent, 17.9 percent, and 7.9 percent under scenarios A1B, A2, and B1, respectively, during the same period. Projected increases in TP flux under all scenarios are consistently smaller than those for TN flux because of the lack of an atmospheric source of phosphorus. The effects of population and developed land growth on TN are compounded by associated increases in the atmospheric sources, which are an important source in many basins in the Eastern United States. Moreover, rising population and urban development under all scenarios tended to have the greatest influence on the coastal flux of both nutrients and is most pronounced outside of the Gulf of Mexico drainage.

6.4.1.3. Total Suspended Sediment

The baseline TSS flux to the five coastal regions averaged 416.5 Tg/yr (fig. 6–7; table 6–3). Similar to TN and TP, the Gulf of Mexico drainage produced 87 percent of TSS, the three east coast regions together contributed 10 percent, and the Great Lakes region contributed about 3 percent. In contrast to the patterns for TN and TP, however, the large TSS yield from the Gulf of Mexico drainage (74,900 kilograms per square kilometer per year (kg/km^2/yr)) was highest among the five regions due to large areas of erodible cropland in the basin (table 6–4). Lowest in yield terms were the Gulf of Maine and Great Lakes regions (25,397 kg/km^2/yr and 37,769 kg/ km^2/yr, respectively) due to large areas of less erodible forest and pasture in those regions.

The estimated TSS flux from all five regions was projected to increase between 4 percent and 53 percent by 2050 under scenarios A1B and A2, with the largest increases in the South Atlantic Bight region (fig. 6–8; table 6–3). In all regions, urban development contributed most to increases in TSS. By contrast, under scenario B1, greater environmental and biodiversity protection than in scenario A1B or A2 results in a smaller increase in the land area devoted to urban development; consequently, an increase in sources from agricultural lands explained a greater fraction of the increase (nearly one third) than under other scenarios. Hence, TSS flux to the five coastal regions is projected to increase by smaller percentages under scenario B1 than under either scenario A1B or scenario A2.

6.4.1.4. Total Organic Carbon

The baseline (2005) coastal flux of TOC from the five regions was 18.5 Tg/yr (table 6–3). Seventy-four percent originated in the Gulf of Mexico drainage, 18 percent originated in the combined east coast drainages, and 8 percent originated in the Great Lakes drainage (fig. 6–9). The South Atlantic Bight part of the east coast drainage had the highest yield (5,665 kg/km^2/yr) due to large wetland and forest sources (table 6–4), and relatively short travel distances to the east coast. Other regions with high delivered TOC yield were the Mid-Atlantic Bight (4,201 kg/ km^2/yr) and Great Lakes (3,709 kg/km^2/yr) drainages and stem from the extensive forest cover and relatively short travel distances in the basin. The Gulf of Mexico drainage had the lowest yield (2,830 kg/km^2/yr) due to longer travel times and larger in-stream losses than in any other region of the Eastern United States.

Predicted increases in TOC flux by 2050 for the five regions were small, ranging from 0.8 to 6.3 percent among the three scenarios (fig.6–10). These changes are significantly smaller than those projected for TN, TP, and TSS and reflect the fact that changes in forest and wetland cover were predicted to be generally small under all scenarios. The largest changes in TOC in the five regions were predicted under scenario B1 (3.9 percent overall increase) because efforts to reverse urban development and nurture natural areas led to more modest predicted increases in wetland areas (chap. 2). For example, coastal TOC flux from wetlands in the Gulf of Mexico drainage was projected to increase by about 6 percent under scenario B1, whereas, coastal TOC flux was predicted to decrease by 5 percent under scenario A1B.

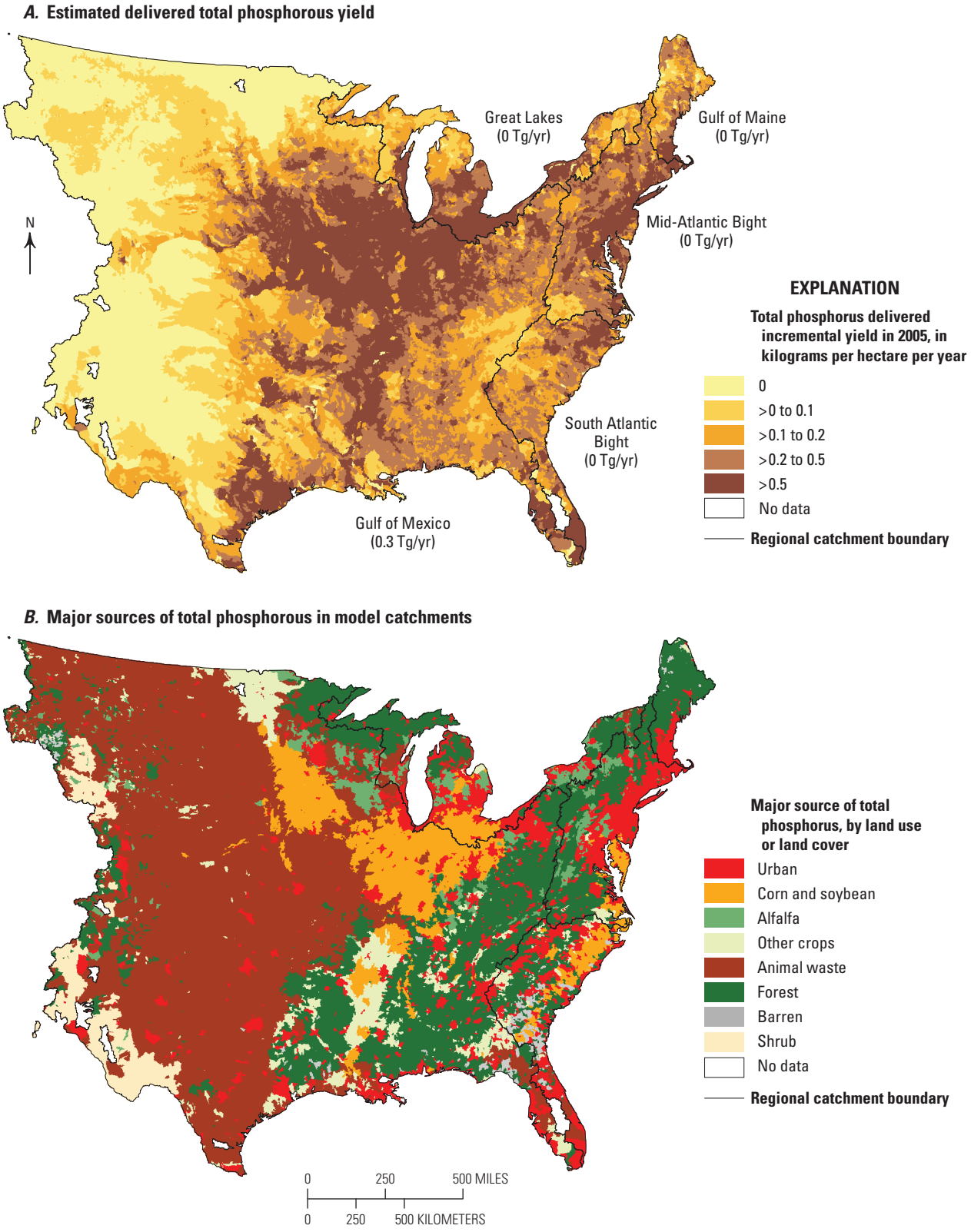

Figure 6–5. Maps showing *A*, estimated delivered total phosphorus (TP) yield to coastal waters and *B*, major sources of TP in model catchments under baseline (2005) conditions in the Eastern United States. Delivered yield reflects the effects of in-stream losses that occur during transport from the outlet of a catchment through the stream and river system to coastal waters. Values shown in parentheses indicate net flux of TP for each region. Tg/yr, teragrams per year; >, more than.

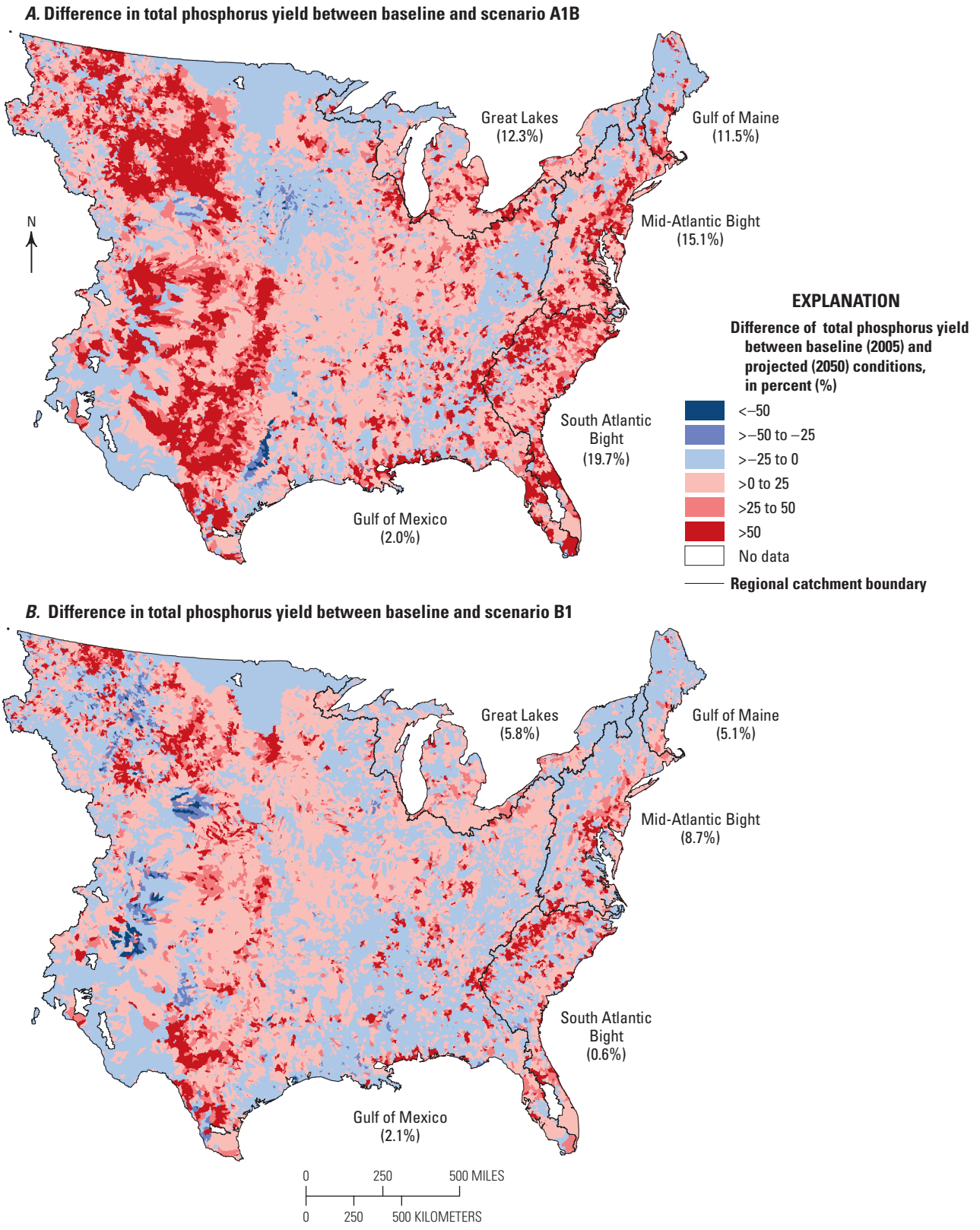

Figure 6–6. Maps showing difference between estimated delivered total phosphorus (TP) yield to coastal waters under baseline (2005) conditions and projected (2050) conditions for Intergovernmental Panel on Climate Change Special Report on Emissions Scenarios (SRES; Nakićenović and others, 2000) scenarios *A*, A1B and *B*, B1 in the Eastern United States. Values shown in parentheses indicate regional difference from baseline. <, less than; >, more than.

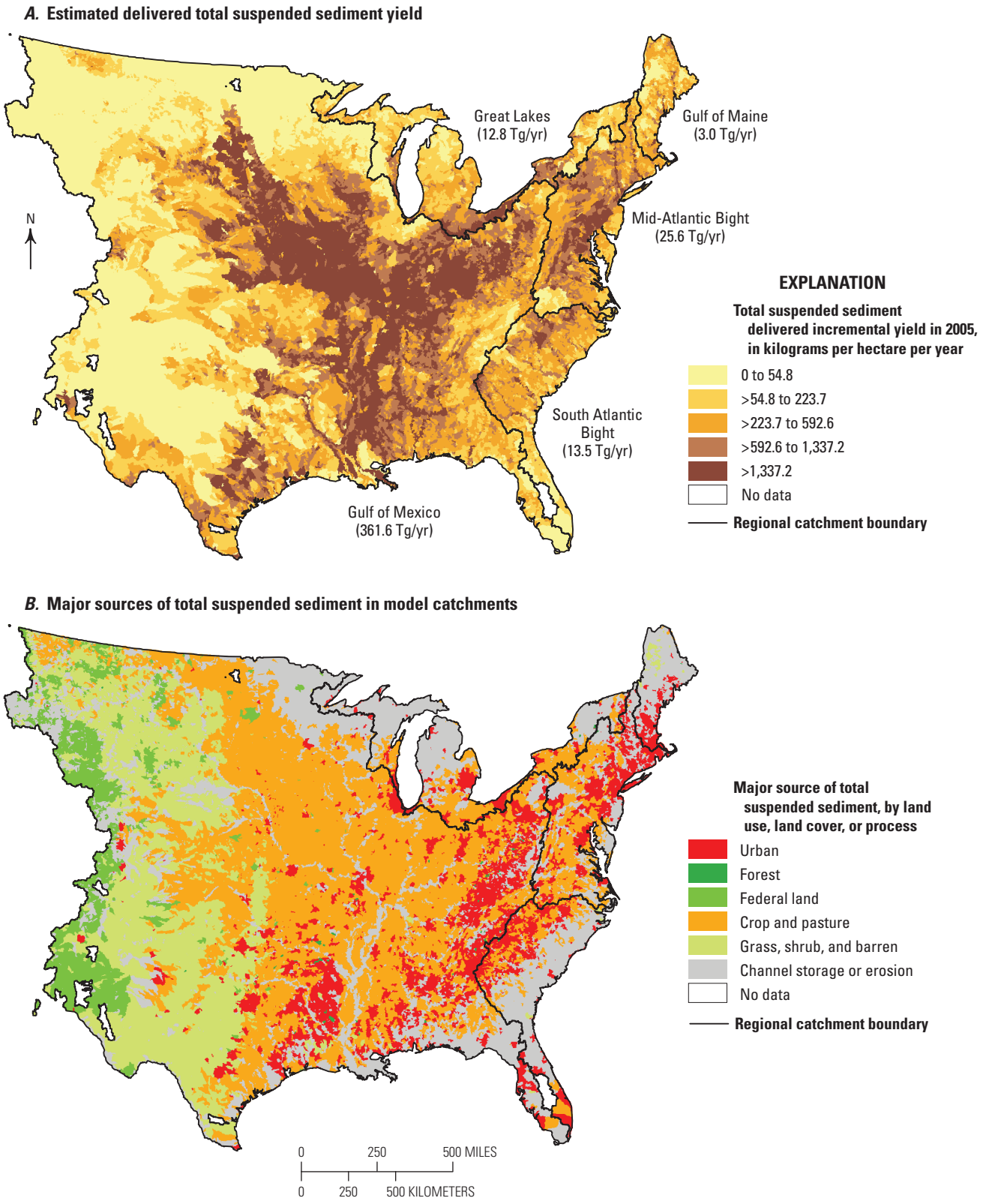

Figure 6–7. Maps showing *A*, estimated delivered total suspended sediment (TSS) yield to coastal waters and *B*, major sources of TSS in model catchments under baseline (2005) conditions in the Eastern United States. Delivered yield reflects the effects of in-stream losses that occur during transport from the outlet of a catchment through the stream and river system to coastal waters. Values shown in parentheses indicate net flux of TSS for each region. Tg/yr, teragrams per year; >, more than.

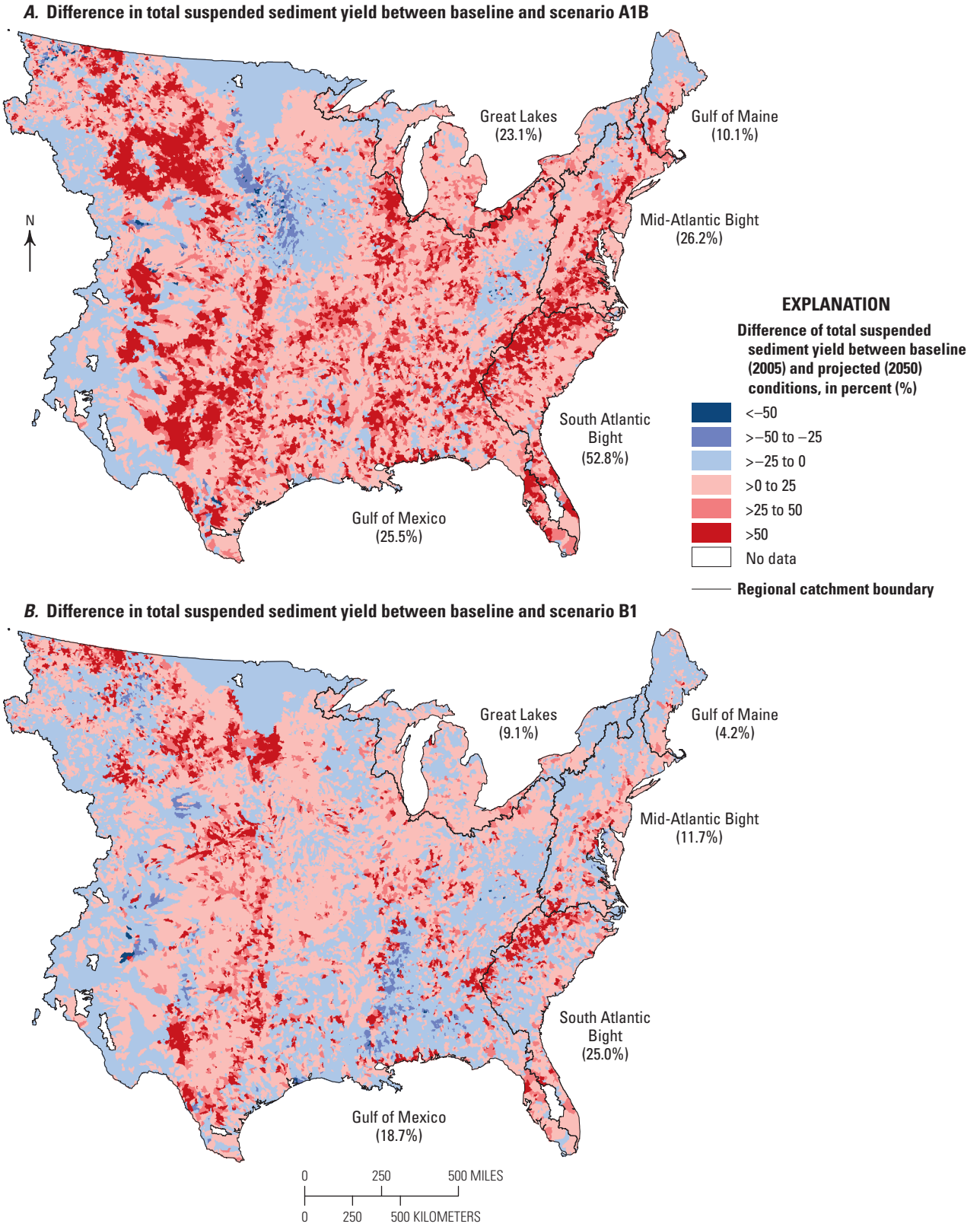

Figure 6–8. Maps showing difference between estimated delivered total suspended sediment (TSS) yield to coastal waters under baseline (2005) conditions and projected (2050) conditions for Intergovernmental Panel on Climate Change Special Report on Emissions Scenarios (SRES; Nakićenović and others, 2000) scenarios *A*, A1B and *B*, B1 in the Eastern United States. Values shown in parentheses indicate regional difference from baseline. <, less than; >, more than.

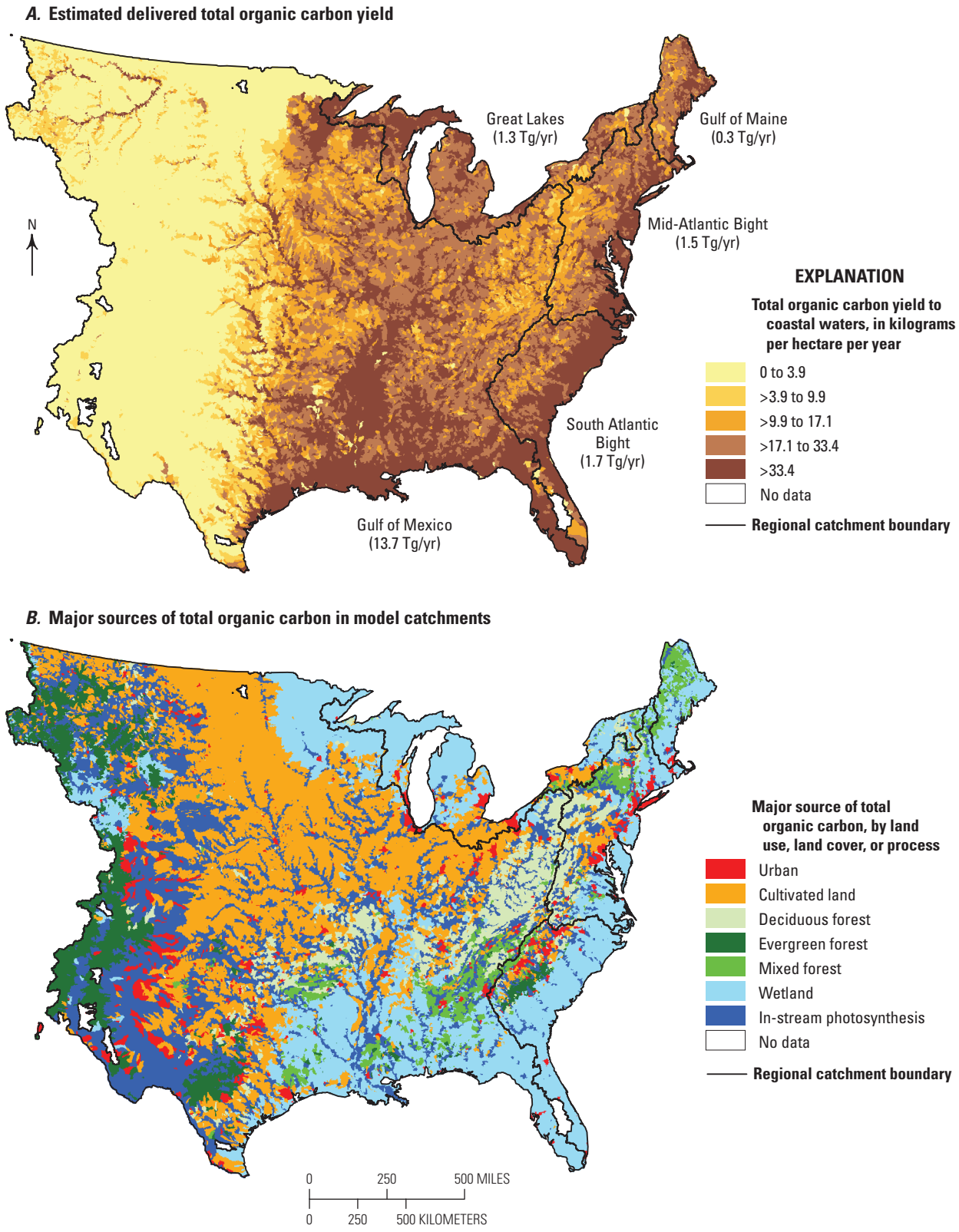

Figure 6–9. Maps showing *A*, estimated delivered total organic carbon (TOC) yield to coastal waters and *B*, major sources of TOC in model catchments under baseline (2005) conditions in the Eastern United States. Delivered yield reflects the effects of in-stream losses that occur during transport from the outlet of a catchment through the stream and river system to coastal waters. Values shown in parentheses indicate net flux of TOC for each region. Tg/yr, teragrams per year; >, more than.

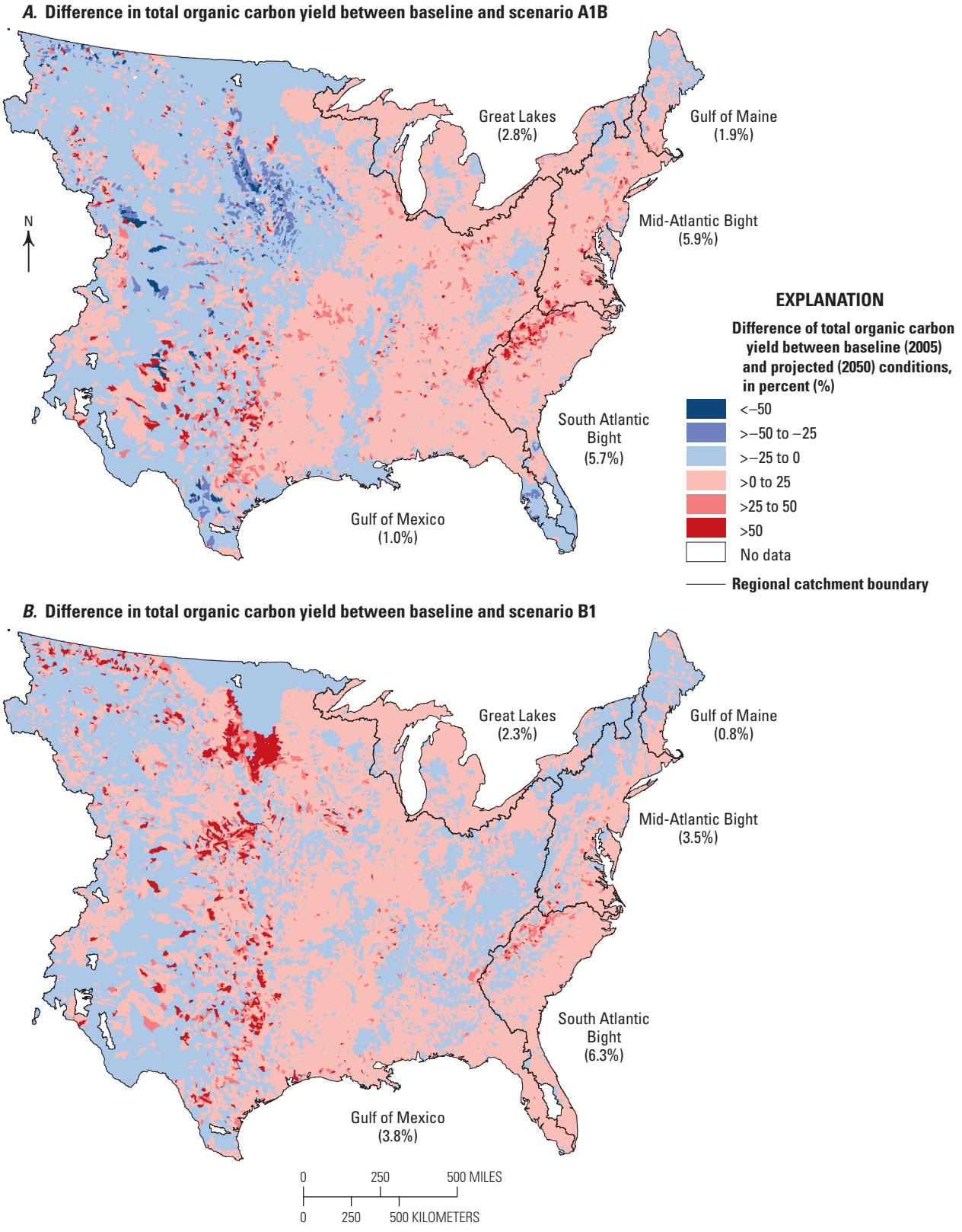

Figure 6–10. Maps showing difference between estimated delivered total organic carbon (TOC) yield to coastal waters under baseline (2005) conditions and projected (2050) conditions for Intergovernmental Panel on Climate Change Special Report on Emissions Scenarios (SRES; Nakićenović and others, 2000) scenarios *A*, A1B and *B*, B1 in the Eastern United States. Values shown in parentheses indicate regional difference from baseline. <, less than; >, more than.

6.4.2. Carbon Storage in Coastal Waters

The coastal model used the adjusted nutrient and sediment inputs to estimate the millennial C_T storage rates in coastal waters—burial in sediments and storage in deep ocean waters. This provides an estimate of the amount of CO_2 removed from the atmosphere into coastal oceans that is specifically attributable to the terrestrial fluxes of nutrients and sediments. The model also estimated burial rates across the entire domain to facilitate comparisons to regional sediment carbon budgets. Finally, the "active" sedimentary inventory of C_T was also estimated as the mass of C_T in the upper 1 m of sediment (Hedges and Keil, 1995) using burial conditions based on the fluxes in the baseline year. This was done to permit comparisons to terrestrial soil carbon and biomass carbon pool size estimates (chap. 7).

6.4.2.1. Estuary Retention and Denitrification

The SPARROW-modeled fluxes of nutrients and sediments were converted to annual rates of carbon storage in sediments and in the deep ocean by separately estimating primary production, sediment burial, and remineralization in the deep ocean using the model framework described above. However, the SPARROW fluxes were adjusted for retention within estuaries before being used in the coastal C_T storage model because the SPARROW model typically ends at the last nontidal reach. Sediment and phosphate retention in estuaries rates ranged up to 63 percent in the Chesapeake Bay, with an average of 11 percent among major estuaries (those in the NEEA database). TN retention rates in estuaries ranged up to 50 percent in Chesapeake Bay and averaged 22 percent among major estuaries. The information available to calculate retention in the Great Lakes region was insufficient, so median values for retention in coastal estuaries were used.

Similarly, an adjustment for nitrogen loss due to diffusive denitrification was also made to the SPARROW fluxes before use in the model. Modeled nitrogen loss ranged from 4.3 percent in the Gulf of Maine to 11 percent in the South Atlantic Bight. The effective estimated rates of diffusive denitrification in shallow waters ranged up to more than 1,000 mmol/m^2/yr, which was consistent (on an areal basis) with literature estimates (Seitzinger and Giblin, 1996; Piña-Ochoa and Alvarez-Cobelas, 2006). It should be noted that, as a sink for nitrogen, diffusive denitrification represents the lesser of the two ways denitrification was accounted for in the model.

6.4.2.2. Coastal C_T Storage

Storage of C_T in coastal waters of the Eastern United States was estimated to be 7.8 Tg/yr for the baseline year. This is roughly four times the C_T storage estimate for coastal waters Pacific United States, calculated using similar methods (Zhu and others, 2010). The Gulf of Mexico alone accounted for 79 percent of the total C_T for the Eastern United States, or about three times the C_T storage of the Pacific United States, owing to the large flux of nutrients and sediments from the Mississippi River. High nutrient and suspended sediment fluxes originating from the Mississippi River resulted in high model estimates of primary production and high burial efficiencies, magnifying the C_T storage in shallow gulf coast waters.

Much of the modeled C_T storage in the Gulf of Mexico was due to burial near the mouth of the Mississippi River, with the highest modeled burial rates near the Mississippi River Delta (fig. 6–11). This is consistent with global assessments showing that the majority of carbon stored in coastal sediments is found in large river deltas (Hedges and Keil, 1995). The model also showed that burial along the coastline to the west of the Mississippi and along the coast of western Florida were important (fig. 6–11). The influence of fluxes from the Mississippi River on modeled C_T storage extended to the western model boundary and offshore all the way to the 2,000-m boundary (figs. 6–2 and 6–11). High burial rates along the coast west of the Mississippi River are consistent with high carbon accumulation rates and high modern content of carbon observed in this region (Gordon and others, 2001; Turner and others, 2007; Sampere and others, 2008). Along the coastline of western Florida, modeled C_T storage rates decreased as the shelf becomes wider and as TN, TP, and TSS concentrations decreased. As a result, 58 percent of C_T stored in the gulf coast region was buried in the sediments; 84 percent of this burial was at water depths less than 200 m.

Nevertheless, it should be noted that, despite the high burial in shallow zones near the mouth of the Mississippi River, modeled C_T storage in the deep ocean for the Gulf of Mexico represented 42 percent of the total storage, largely in the deeper areas of the northeastern gulf coast (fig. 6–11). This highlights the importance of bathymetry in determining C_T storage. Deep waters have a disproportionately large influence on carbon storage rates because transport of primary production below the deep mixed layer and into deep ocean waters is the most efficient form of C_T storage in the model. Remineralization within sediments during burial reduces the amount of carbon stored considerably compared areas of similar productivity over deep water. In areas of low sediment flux, calculated burial efficiencies were near zero.

For the eastern seaboard, total modeled C_T storage was 1.3 Tg/yr (table 6–4), accounting for about 17 percent of the total for the Eastern United States. C_T storage along the east coast was about 36 percent lower than that of the Pacific coast, corresponding to lower nutrient and sediment fluxes on the east coast. The sediment, terrestrial carbon and nutrient fluxes on the east coast were also much lower than for the Gulf of Mexico, but the contrast in modeled C_T storage was even greater; although the nutrient flux along the eastern seaboard comprised one third of the gulf coast nutrient flux, C_T storage in the eastern seaboard was only one fifth as large as that of the gulf coast. This lower relative C_T storage was due largely to lower relative suspended sediment flux in the region (about 5 percent), which resulted in lower modeled burial efficiencies. Similar to the Gulf of Mexico, regional bathymetry played

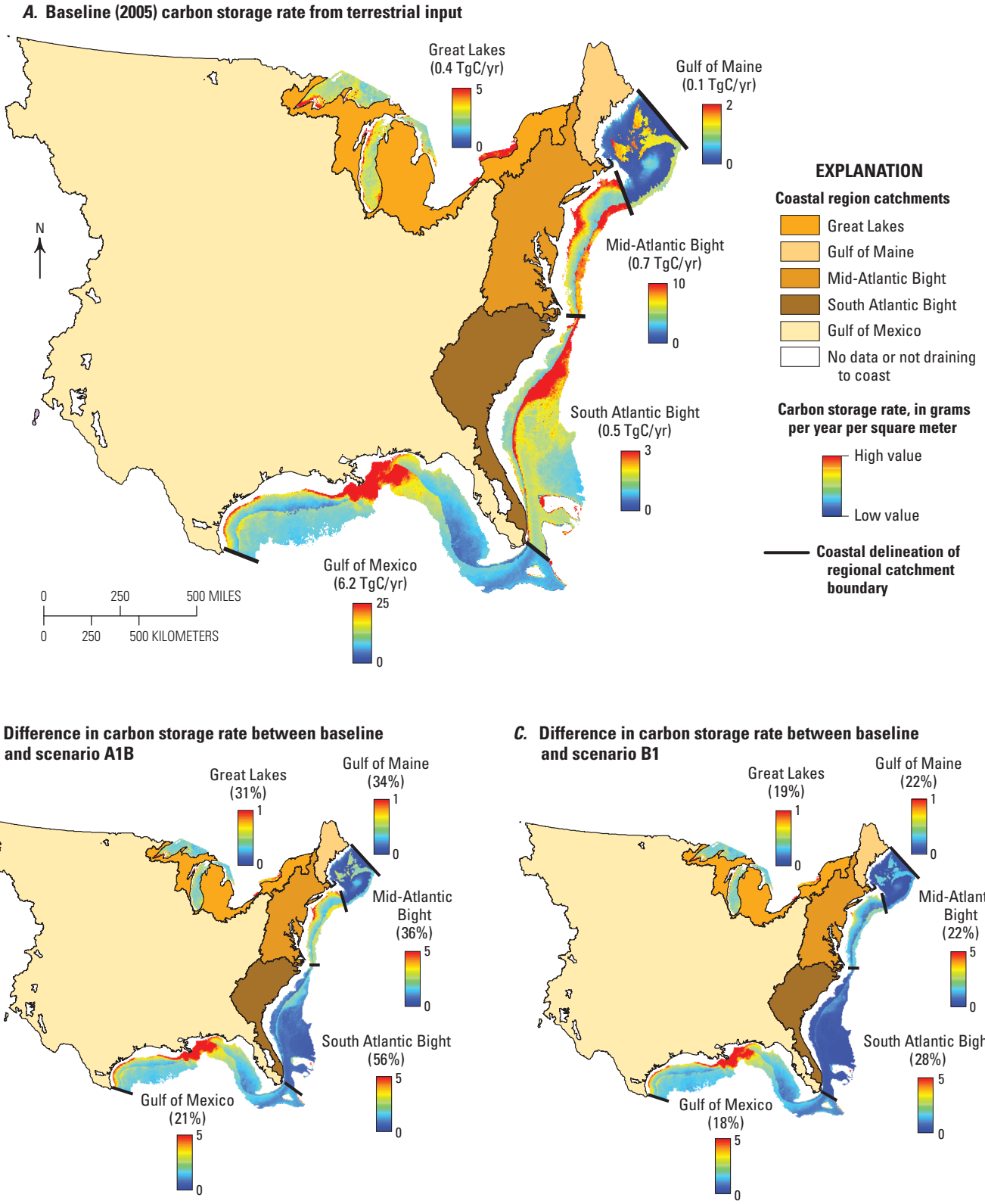

Figure 6–11. Maps showing model-derived millennial carbon storage rates for carbon storage directly attributable to terrestrial inputs (C_T) in coastal waters *A*, under baseline (2005) conditions and as differences for projected (2050) conditions based on Intergovernmental Panel on Climate Change Special Report on Emissions Scenarios (SRES; Nakićenović and others, 2000) scenarios *B*, A1B and *C*, B1 in the Eastern United States. Values shown in parentheses indicate total carbon storage rate *A*, for each region or *B* and *C*, as a difference for each region. Color scales are unique to each region. TgC/yr, teragrams of carbon per year; %, percent.

an important role; a shallower average bathymetry along the eastern seaboard resulted in a greater proportion of C_T storage as burial rather than deep ocean storage.

There is considerable bathymetric diversity among the eastern seaboard regions; whereas the South Atlantic Bight has relatively steep bathymetric gradients, the Mid-Atlantic Bight has relatively broad shallow bathymetry, and the Gulf of Maine and Great Lakes have irregular bathymetric gradients. Modeled storage of C_T in the deep (more than 200 m) offshore waters was dominant in the South Atlantic Bight, accounting for 75 percent of C_T storage as DIC in deep waters (remineralized remains of the phytoplankton production from the surface ocean) in the South Atlantic Bight. By contrast, sediment C_T burial in the relatively shallow bathymetry of the Mid-Atlantic Bight accounted for 73 percent of total C_T; much of the C_T stored in the Mid-Atlantic Bight was buried in shallow shelf sediments rather than stored in deep ocean waters.

There was considerable diversity in modeled C_T storage among the physiographic regions on the eastern seaboard due to bathymetric differences as well as differences in sediment and nutrient inputs. The highest rates of coastal C_T storage were in the Mid-Atlantic Bight, which accounted for 57 percent of the total, followed by the South Atlantic Bight (37 percent) and the Gulf of Maine (6 percent). The higher rates of C_T storage in the Mid-Atlantic Bight were attributable primarily to elevated modeled primary production resulting from high nutrient inputs (fig. 6–11; table 6–3). The Mid-Atlantic Bight had the highest modeled terrestrial organic carbon and nutrient inputs, largely due to the higher population and urban land use in the Hudson River Basin and the Chesapeake Bay (figs. 6–3 and 6–5; table 6–4; Malone and others, 1996; Gibson, 1998). These inputs were elevated in the coastal ocean despite the comparatively high modeled estuarine C_T retention in the Mid-Atlantic Bight.

The lowest modeled C_T storage rates in the Eastern United States were in the Gulf of Maine (6 percent; fig. 6–11). Terrestrial organic carbon and nutrient flux was nearly five times lower in the Gulf of Maine compared with the Mid-Atlantic Bight and only half as much in the South Atlantic Bight, resulting in lower modeled primary production and C_T storage. Reduced riverine suspended sediments entering the Gulf of Maine compounded the effect of lower nutrient flux by contributing to reduced burial efficiencies and C_T burial rates in shallow waters (table 6–3). Further, the variable bathymetry of the Gulf of Maine resulted in a higher proportion of C_T storage (43 percent) through burial rather than through transport to the deep ocean relative to other regions (fig. 6–11).

The Great Lakes accounted for about 5 percent of the total modeled C_T storage in the Eastern United States (table 6–3), driven by nutrient and sediment dispersion among the lakes. In contrast to the other regions, there was no permanent deep mixed layer under which CO_2 is presumed to accumulate and thus contribute to total C_T storage; all storage is through sediment burial. Consequently, the effects of bathymetry in model results were less important than for the other regions, and burial efficiency was the primary determinant of C_T storage. Maximum modeled rates of burial were in Lake Ontario, followed by the small deep basin of eastern Lake Erie and the shorelines of eastern Lake Michigan and southern Lake Superior (fig. 6–11), although the assessment extends only to the border of the United States. All these areas are characterized by dense population and high levels of urban and agricultural lands use, characteristics that lead to elevated riverine export of nutrients and total suspended sediment (table 6–4). Relatively little C_T storage was found to occur in the deep waters of northern Lake Huron where low watershed population densities and agricultural lands use correspond with relatively low riverine terrestrial organic carbon, nutrient, and sediment inputs.

6.4.2.3. Sediment C_T Inventory

Organic carbon in the upper meter of sediment is considered one of the primary "active" pools of carbon storage in the marine system and can be considered a rough analog of the terrestrial soil organic carbon pool that is commonly used in comparisons and aggregations of active carbon pools (Hedges and Keil, 1995). Based on the results of the model, the integrated total mass of C_T that would accumulate as a pool of carbon in the upper meter of sediment under baseline flux conditions from the Eastern United States is 9,100 teragrams (Tg; fig. 6–12; table 6–3), which represents one third of terrestrial carbon pools (chap. 7). However, the distribution of this sediment C_T "inventory" among the coastal regions was different from the distribution of storage rates (fig. 6–3), highlighting the importance of burial rates in determining the long-term sediment repository for carbon. For example, the majority of C_T inventory of coastal sediments in the Eastern United States was in the sediments of the eastern seaboard, whereas the highest rates of C_T storage were in the Gulf of Mexico. The modeled C_T inventory of the eastern seaboard was about 4,000 Tg (fig. 6–12) compared with about 2,300 Tg for the Gulf of Mexico and 2,900 Tg for the Great Lakes.

There are two main reasons why the distribution of sediment C_T inventory does not correspond to the rates of storage. First, the sediment C_T inventory is dependent on the percentage of organic carbon in buried sediments, which is determined by the local sediment flux, the ratio of productivity to sediment flux, and the bathymetry. Very high inorganic sediment fluxes can result in dilution of the organic carbon buried (Tyson, 2001). Second, the modeled C_T storage rate is not simply a function of the burial rate. Rather, it is the sum of the burial rate and the accumulation rate of remineralized C_T in the deep ocean water, which can be substantial. For example, despite the high rates of sediment burial, a significant amount of carbon is also stored as DIC in the deep ocean waters (more than 200 m) of the Gulf of Mexico, the result of remineralization combined with the steep bathymetry of the northeastern Gulf of Mexico (fig. 6–1).

The allocation of total C_T storage rates between sediment burial and storage in deep ocean water as DIC provides a

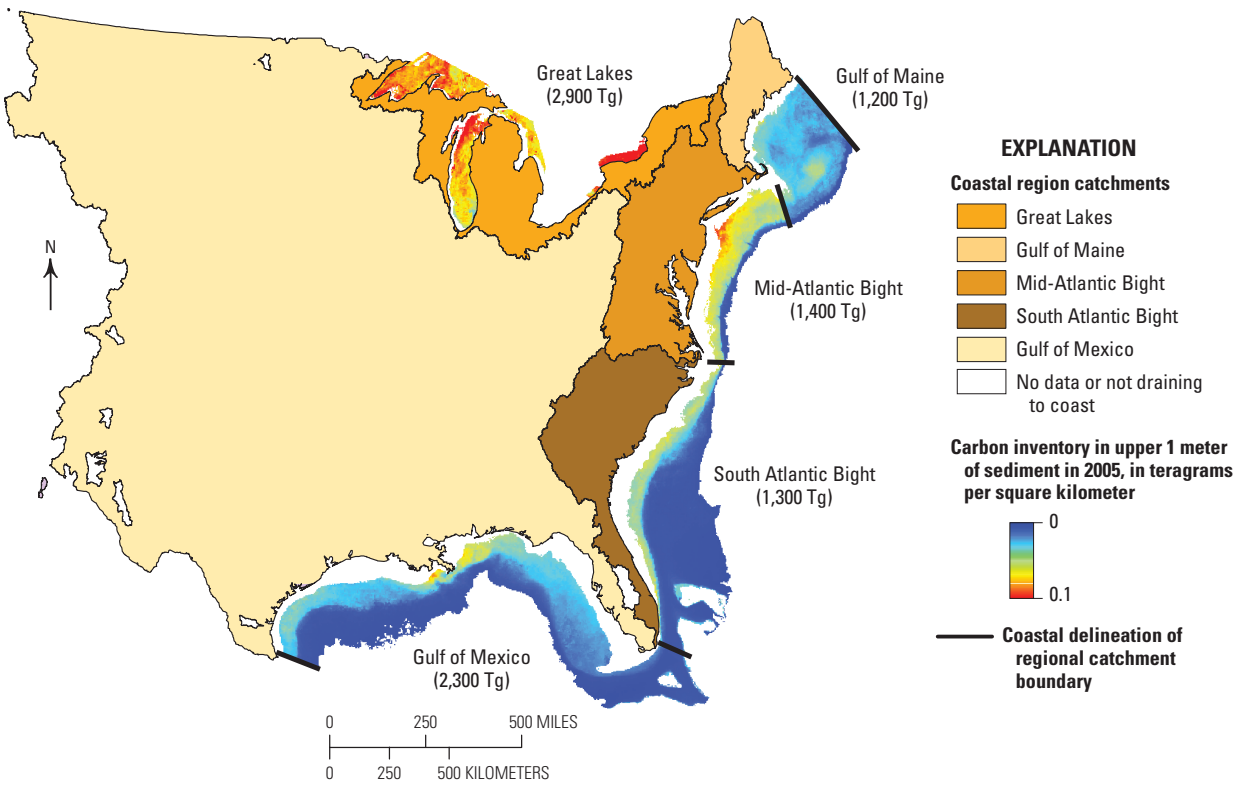

Figure 6–12. Map showing estimated inventory of carbon directly attributable to terrestrial inputs (C_T) that would be stored in the upper 1 meter of sediment under baseline (2005) flux conditions in the Eastern United States. Values shown in parentheses indicate total carbon storage for each region. Tg, teragrams.

means to crudely assess the carbon inventory accumulated in both pools together for the time during which the upper 1 m of sediment accreted. Assuming that this ratio, which is largely determined by bathymetry, is consistent for the period of deposition, an amount of carbon equivalent to two thirds of buried carbon is stored as DIC in the deep ocean. This suggests that, under baseline flux conditions, a total C_T inventory of nearly 15,000 Tg would result. This represents a pool size more than half the estimated size of the terrestrial carbon pool (26,962 TgC) and about equal to the size of the terrestrial soil carbon pool (chap. 7).

However, the time scales of carbon accumulation in these two pools are very different. The rate of carbon accumulation as well as the rate of response to change are much lower in coastal systems than in terrestrial systems (Sarmiento and Gruber, 2002). The C_T burial rate in marine sediments (4.7 Tg/yr) is far less than that in terrestrial soils (65.4 Tg/yr; chap. 7). The C_T storage rate in coastal waters of the Eastern United States total is only 3 percent of the estimated terrestrial flux (chap. 7).

6.4.2.4. Projected Changes in C_T Storage in Coastal Waters

C_T storage and burial rates in coastal systems increased under all three modeled SRES scenario LULC projections. The projected future rise in C_T storage rate was driven by substantially elevated nutrient and sediment fluxes, which interact synergistically to increase modeled carbon storage rate. The relative changes in these fluxes and in carbon storage rate was highest for SRES scenario A1B, with rates of carbon storage in the Eastern United States projected to increase by an average of 25 percent by 2050. The South Atlantic Bight showed the highest increase (56 percent), followed by the Mid-Atlantic Bight (36 percent), the Gulf of Maine (34 percent), the Great Lakes (31 percent), and the Gulf of Mexico (21 percent). Scenario B1 had the lowest projected rise in C_T storage rate of the three scenarios tested, with the average storage rate in 2050 estimated to be 19 percent higher than the baseline; this was still only about 76 percent of the increase projected for scenario A1B (with a similar proportional change between regions).

The amount of change in C_T storage rates (fig. 6–11) reflects the spatial variability and relative change in urban, agricultural, and atmospheric sources (figs. 6–3, 6–5, 6–7, and 6–11; table 6–4). The projected changes in C_T storage rates under all SRES scenarios were greatest in the eastern seaboard, particularly in the South Atlantic Bight. This was largely the result of large projected increases in nutrient and total suspended sediment flux to coastal waters, but these increases were exacerbated by relatively low watershed and estuarine retention and steep increases in the depth of coastal waters. Although the Gulf of Mexico dominated

total C_T storage rates in the Eastern United States due to the large fluxes of nutrients and suspended sediments from the Mississippi River, the increase in these fluxes compared with the baseline flux was low for all scenarios tested. Because the Mississippi River sediment and nutrient fluxes account for about 80 percent of the input to coastal waters for the Eastern United States, the aggregate average increase for the Eastern United States as a whole is biased toward the low projected change in the Gulf of Mexico.

The projected changes in C_T storage rates under scenario B1 were smaller than those estimated for scenarios A1B and A2 (fig. 6–11; table 6–3) because less land area is devoted to urban development under scenario B1 (fig. 6–5). This resulted in a lower nutrient and suspended sediment flux for scenario B1 than for scenario A1B, particularly along the eastern seaboard where there are many major population centers. Although relative differences in C_T storage projections for scenario B1 were greatest on the eastern seaboard, the differences between regions were less than for the other scenarios (fig. 6–11), indicating that the differences in patterns of development and land use embodied in the different scenarios can substantially affect coastal C_T storage rates, thereby altering the carbon cycle of the ocean significantly.

6.4.3. Summary of Carbon Storage Related to Coastal Processes

The majority of the portion of coastal carbon storage directly related to terrestrial processes in the Eastern United States resulted from the burial of organic carbon in sediments rather from than transport and storage in the deep ocean. However, transport to the deep ocean was also significant and was more sensitive to projected changing inputs. Of the total carbon stored, the model results suggested that about 60 percent of the coastal C_T was buried in coastal sediments, whereas about 40 percent was stored as carbonate in deep ocean waters. The rate of C_T storage was about 3 percent of the rate of terrestrial carbon storage, but the amount of C_T that would be stored in the active coastal carbon pools under baseline flux conditions was on the same order as that stored in terrestrial carbon pools because of the longer timescales of carbon accumulation in the ocean compared with carbon accumulation by terrestrial processes.

Coastal bathymetry plays an important role in coastal carbon storage. Deep areas export primary production beneath the deep mixed layer, keeping dissolved inorganic carbon produced as a consequence of remineralization isolated from exchange with the atmosphere and resulting in relatively reduced remineralization rates upon organic carbon burial. By contrast, shallow regions, even those with high incident sediment loads, tend to bury more of their production, which is less efficient because the continued slow degradation in shallow (less than 200 m) sediments results in return of the remineralized carbon to the atmosphere.

According to the model, the amount of C_T buried in sediments was partitioned by water depth as follows: 38 percent was buried in waters less than 50 m deep, 32 percent was buried between 50 m and 100 m deep, 15 percent was buried between 100 and 200 m deep, and the remainder (about 15 percent) was stored in sediments more than 200 m deep. The decreased burial in the deep zones was because of the low sediment flux in this region and the remineralization that occurs during settling through a deep-water column. These results agree with Dunne and others (2007), who suggested that previous ocean models of carbon storage rates did not account for the appreciable carbon storage that occurs in shallow coastal sediments.

C_T storage in coastal waters was found to be sensitive to projected changes in fluxes of sediment and nutrients to coastal waters. Under all scenarios modeled, carbon storage in coastal systems was projected to increase. The projected increase in carbon storage is driven by substantially elevated projected nutrient fluxes and elevated sediment fluxes. These two fluxes interact synergistically to increase modeled carbon storage. Projections for scenario A1B exhibited the greatest proportional change in coastal C_T storage. Rates of total carbon storage for the Eastern United States were projected to increase by 25 percent for this scenario; the South Atlantic Bight showed the highest increase (56 percent), followed by the Mid-Atlantic Bight, the Great Lakes, the Gulf of Maine, and the Gulf of Mexico. Changes in C_T storage in the Gulf of Mexico were primarily driven by changes in sedimentation, whereas the changes in the east coast and the Great Lakes were driven primarily by changes in population density and corresponding increases in nutrient and total suspended sediment transport via rivers to coastal waters.

6.5. Conclusions and Implications

Coastal ocean primary productivity has been changing in response to increased nutrient loading. Increased primary production (Herbert, 1999) and fisheries landings (Breitburg and others, 2009) and a greater areal extent of hypoxia resulting from terrestrial inputs (Bianchi and others, 2010) are well documented. The model results presented in this report project a continued increase in nutrient fluxes associated with increasing population and agricultural intensity (Howarth, 2008). This continued increase has important implications for management of coastal resources because of the increased incidence of coastal and estuarine hypoxia (Bianchi and others, 2010) and harmful algal blooms (Anderson and others, 2002; Glibert and others, 2005). Increased areas of hypoxic sediments will likely increase the rates of carbon storage (Bergamaschi and others, 1997; Middelburg and Levin, 2009).

This assessment highlights the notion that processes controlling carbon storage in coastal oceans are not in steady state; rates of nutrient and sediment input are continuously changing in response to land use modification and population increase, among the many other drivers of change. A debate exists in the published literature regarding whether a change in coastal carbon burial rates has been or will be observed

in coastal sediments. Walsh and others (1985) believe that population and land use change have already led to increased coastal carbon burial rates. The Arabian Sea Carbon Flux Group and others (Lee and others, 1998) found evidence of changes to sediment burial due to anthropogenic activity in waters off the Pacific coast. Middelburg and Levin (2009) summarized the geochemical evidence for the levels of increased carbon preservation in coastal sediments that may be expected. Alternatively, some studies have found that modern carbon burial rates are similar to long-term rates, and thus no change has occurred; no evidence of recent changes in carbon burial rates was found in east coast sediments (Alperin and others, 2002; Thomas and others, 2004) or in the Gulf of Mexico (Allison and others, 2007). The results of the current study suggest that changes in C_T burial—the part of the burial rate subject to change—are spatially variable and potentially obscured by competing processes. Changes in sediment carbon burial rates may be due to changes in phytoplankton production as well as sediment delivery, with elevated sediment delivery potentially leading to a reduced organic content rather than enrichment because of dilution (Tyson, 2001). The location of studies intended to document changes resulting from altered terrestrial fluxes must be carefully chosen to focus on the nutrient or sediment supply only.

This assessment underscores the need for progress in our understanding of carbon storage in coastal systems. Although there have been significant strides in understanding the role of denitrification and other nitrogen cycling processes in the coastal ocean, there is a high degree of uncertainty about the relative importance of different processes (Seitzinger and others, 2006; Burgin and Hamilton, 2007; Trimmer and Engström, 2011). Large-scale datasets that permit simple model synthetic reproduction are not available. Additional research in coastal nutrient cycling is necessary to accurately evaluate the effects of changing continental fluxes.

Finally, this assessment also highlights the need for a greater understanding of carbon storage and cycling in estuarine sediments. C_T and the total inventory of carbon in estuaries was assumed to be constant in this assessment because no models were available to relate carbon burial efficiency in estuaries to sediment accumulation rates and because remote sensing data still cannot be interpreted reliably in these areas. Furthermore, based on a simple empirical model formulation, the results of this assessment indicate that sediment carbon burial rates in estuaries represent 1 to 6 percent of total coastal carbon storage rates. However, this is likely an underestimate because it presumes no long-term carbon sequestration. A clearer picture of carbon accumulation in estuaries is important for understanding the effects and mechanisms of estuarine processing that influence terrestrial efflux and coastal carbon storage.